Atmos. Chem. Phys., 25, 16945–16968, 2025 https://doi.org/10.5194/acp-25-16945-2025 © Author(s) 2025. This work is distributed under the Creative Commons Attribution 4.0 License.





A nitrate photolysis source of tropospheric HONO is incompatible with current understanding of atmospheric chemistry

Matthew J. Rowlinson^{1,2}, Lucy J. Carpenter¹, Mat J. Evans¹, James D. Lee^{1,2}, Simone T. Andersen³, Tomas Sherwen⁴, Anna B. Callaghan¹, Roberto Sommariva⁵, William Bloss⁵, Siqi Hou⁵, Leigh R. Crilley⁶, Klaus Pfeilsticker⁷, Benjamin Weyland⁷, Thomas B. Ryerson⁸, Patrick R. Veres^{9,a}, Pedro Campuzano-Jost¹¹, Hongyu Guo¹³, Benjamin A. Nault^{12,13}, Jose L. Jimenez^{10,11}, and Khanneh Wadinga Fomba¹⁴

Birmingham, B15 2TT, UK

⁶Atmospheric Services, WSP Australia, Brisbane, Australia

⁷Institute of Environmental Physics, University of Heidelberg, Heidelberg, Germany ⁸National Oceanic and Atmospheric Administration (NOAA), Chemical Sciences Laboratory (CSL), Boulder, CO, USA

⁹Chemical Sciences Division, Earth System Research Laboratory, National Oceanic and Atmospheric Administration, Boulder, CO, USA

NASA Langley Research Center, Hampton, VA, USA
 Cooperative Institute for Research in Environmental Sciences and Department of Chemistry,
 University of Colorado Boulder, Boulder, CO, USA

12 Center for Aerosol and Cloud Chemistry, Aerodyne Research Inc., Billerica, MA, USA
 13 Department of Environmental Health and Engineering, Johns Hopkins University, Baltimore, MD, USA
 14TROPOS – Leibniz-Institute for Tropospheric Research, Permoserstr. 15, 04318 Leipzig, Germany
 anow at: National Science Foundation National Center for Atmospheric Research, Boulder, Colorado, USA

Correspondence: Matthew J. Rowlinson (matthew.rowlinson@hotmail.com) and Mat J. Evans (mat.evans@york.ac.uk)

Received: 21 February 2025 – Discussion started: 26 February 2025 Revised: 2 August 2025 – Accepted: 26 August 2025 – Published: 27 November 2025

Abstract. Recent observations of nitrous acid (HONO) in the remote troposphere show much higher concentrations than can be explained through known sources, with important implications for air quality and climate. Laboratory evidence and modelling of field observations suggests that nitrate aerosol photolysis is the likely mechanism providing the additional HONO, offering a rapid route for recycling of NO_x from nitric acid (HNO₃). Previous studies of the global impact of this chemistry have used either very restricted HONO data or a "top-down" approach to parameterize the HONO source by reconciling simulated and observed NO_x concentrations. Here, we use multiple, independent tropospheric HONO observations from different locations to parameterize nitrate photolysis, and evaluate its impacts on global atmospheric chemistry using GEOS-Chem. The simulations improve agreement between modelled and observed HONO concentrations relative to previous studies, decreasing the model bias by 5%–20%. The remaining (and large) underestimate of HONO in the model is

due predominantly to an underestimate of total nitrate aerosol (-95%) and is reduced to 20% when accounting for low model nitrate. Despite the low bias in the model HONO, we find that nitrate aerosol photolysis leads to substantial global increases in NO_x, O₃ and OH concentrations, likely beyond the observational constraints. The additional source of NO_x (\sim 48 Tg N yr⁻¹ globally) is comparable to total NO_x emissions from all sources (\sim 55 Tg yr⁻¹). These HONO observations in the remote troposphere, thus imply a large uncertainty in the NO_x budget and an incomplete understanding of atmospheric chemistry. Improved techniques to measure HONO at the low concentrations typical of remote areas, coupled with more measurements in these areas and improved process level understanding of nitrate photolysis are needed to provide quantitative assessment of its potentially global-scale atmospheric impacts.

1 Introduction

Nitrogen oxides (NO_x : $NO + NO_2$) and hydroxyl radicals (OH) are crucial drivers and regulators of atmospheric chemistry processes (Monks et al., 2015; Nguyen et al., 2022). NO_x catalyses the production of ozone (O_3) , a significant air pollutant (Monks et al., 2015) and greenhouse gas (Szopa et al., 2021) and modulates the abundance and distribution of OH. OH is known as the atmosphere's "self-cleansing agent" and is the primary oxidant of hydrocarbons, leading to O₃ formation and the production of particulate nitrate aerosol (NO₃⁻), a significant contributor to the atmospheric aerosol load and its radiative effects. Nitrous acid (HONO) is a key species in the cycling between NO_x and HO_x (OH + HO₂) radicals and therefore is also central to regulating tropospheric O_3 (Jiang et al., 2023). NO_x is removed from the atmosphere predominantly by the reaction of OH with NO2 to give nitric acid (HNO₃) or through the hydrolysis of dinitrogen pentoxide (N2O5) on aerosol surfaces to give particulate nitrate (pNO_3^-) (Ramazan et al., 2006; Stavrakou et al., 2013). There is rapid cycling between the gas (HNO₃) and particulate phase nitrate. HNO₃ and pNO₃ are soluble and removed rapidly through wet and dry deposition (Parrish et al., 1986; Meng et al., 1997). HNO₃ can return reactive nitrogen compounds through photolysis or reaction with OH, but these reactions are slow relative to deposition. Conversion of reactive nitrogen oxides to HNO₃ or pNO_3^- has traditionally therefore been considered a terminal sink for reactive nitrogen oxides (Knipping and Dabdub, 2002).

HONO concentrations in the remote atmosphere range from essentially zero up to a few tens of ppt (Ye et al., 2016, 2017, 2023; Reed et al., 2017; Zhu et al., 2022; Andersen et al., 2023; Zhong et al., 2023; Weyland, 2024). For example, observations of HONO at Cabo Verde are typically between 3 and 7 ppt (see Fig. 2 in Reed et al. (2017), and Fig. 2 in this work). During the day HONO has a short photolysis lifetime, of $\sim 600\,\mathrm{s}$ at local noon for Cabo Verde. Conventional understanding is that the dominant gas phase source of HONO is the reaction between OH and NO. Given a noon time NO concentration of ~ 7 ppt (Andersen et al., 2021) and OH concentration $\sim 6\times 10^6\,\mathrm{cm}^{-3}$ (Whalley et al., 2010), the rate of the gas phase production of HONO from the OH + NO re-

action is $\sim 1 \times 10^4 \, \mathrm{cm^{-3} \, s^{-1}}$ which would suggest a steady state HONO concentration (against photolysis) of 0.2 ppt, substantially less than that observed. This implies a large additional source of HONO in these environments.

Various alternative sources of HONO in polluted air masses have been suggested (see for example Yu et al., 2022; Song et al., 2023; Jiang et al., 2024). However, in the clean marine environment, many of these appear to be insufficient to explain the observed HONO. A direct surface source from the ocean is thought to be too small (Crilley et al., 2021). Laboratory experiments show that the heterogeneous uptake of NO2 onto aerosol surfaces releases HONO with reactive uptake coefficient (γ) of $\sim 1 \times 10^{-4}$ (IU-PAC data evaluation at https://iupac-aeris.ipsl.fr/datasheets/ pdf/HET SALTS 4.pdf, last access: 21 November 2025). For an aerosol surface area density typical of Capo Verde $(1 \times 10^{-6} \text{ cm}^2 \text{ cm}^{-3})$, Whalley et al., 2010) and a NO₂ mixing ratio of 20 ppt, this would suggest a steady state HONO concentration of 0.01 ppt. A γ of 0.05 for NO₂ aerosol uptake and conversion to HONO would be necessary for this source to balance the photolysis sink, 3 orders of magnitude more than experimentally determined. Further, the diurnal variation in the HONO concentrations shows a noon maximum and a nighttime minimum (see Fig. 2 in Reed et al., 2017 and Fig. 2 in this work). Given that the NO₂ concentrations do not vary significantly diurnally (Andersen et al., 2021) and there is also likely little diurnal variation in the aerosol concentration, the flux of HONO required from the NO₂ heterogeneous reaction to balance HONO concentrations at noon would suggest much higher HONO concentrations at night than observed. A photo-enhanced uptake of NO₂ might reconcile theory with the observations and has been seen in some laboratory studies on urban grime and on dust (Liu et al., 2019). However, these studies report even lower γ ($\sim 6 \times 10^{-6}$).

Other gas phase mechanisms have been proposed to produce HONO. Crowley and Carl (1997) suggested that electronically excited NO₂ could react with water to yield HONO, but this was shown to be insignificantly slow by Dillon and Crowley (2018). A water mediated production of HONO from the reaction of HO₂ and NO₂ was proposed by Xin et al. (2014). Ye et al. (2015) however, concluded

that this would be a minor channel with only a 3 % HONO branching ratio which would be insufficient to sustain the observed HONO concentrations. Song et al. (2023) proposed a reaction involving NO, HNO₃ and H₂O to increase HONO production, and found that a 2 % yield from the this reaction would be sufficient. However, other experimental evidence for this reaction is currently missing.

There is thus little consensus in the literature on an additional gas phase, NO_x derived source of HONO. There is however a growing body of laboratory and field evidence that particulate phase nitrate (pNO_3^-) can be rapidly photolyzed to produce HONO and NO_2 (with yields x and y; Reaction R1) (Wingen et al., 2008, Ndour et al., 2009; Richards et al., 2011; Richards and Finlayson-Pitts, 2012; Ye et al., 2016; Ninneman et al., 2020; Shi et al., 2021).

$$p\mathrm{NO}_{3}^{-} + h\nu \rightarrow x\mathrm{HONO} + y\mathrm{NO}_{2} \ J_{p\mathrm{NO}_{3}^{-}} \tag{R1}$$

This return of reactive nitrogen compounds from HNO₃ and pNO₃ has been termed "renoxification" (Lary et al., 1997; Bekki, 1997; Ndour et al., 2009), effectively acting as a secondary chemical source of NO_x. Laboratory studies have found that Reaction (R1) occurs 10–1700 times faster than HNO₃ photolysis under atmospheric conditions, typically expressing this rate as an enhancement factor (EF) relative to the rate of HNO₃ photolysis (EF = J_{p NO₃ $^-$ / J_{HNO_3}) (Ye et al., 2016, 2017; Bao et al., 2020; Shi et al., 2021; Sommariva et al., 2023).

Recent field studies have demonstrated that renoxification is a plausible mechanism for the production of HONO measured in the remote oceanic atmosphere (Ye et al., 2016; Reed et al., 2017; Bao et al., 2020; Zhu et al., 2022; Andersen et al., 2023). In these environments , HONO measurements have revealed atmospheric concentrations significantly higher than would be expected from this gas phase chemistry alone (Ye et al., 2016, 2017, 2023; Reed et al., 2017; Zhu et al., 2022; Andersen et al., 2023; Zhong et al., 2023; Weyland, 2024), challenging our understanding of atmospheric chemistry. This renoxification process could therefore represent an important source of NO_x in remote or marine regions where there are few other reactive nitrogen sources (Kasibhatla et al., 2018; Shah et al., 2023).

A number of studies have implemented pNO_3^- photolysis into chemical transport models. Kasibhatla et al. (2018) found that implementing nitrate photolysis on sea-salt aerosols with EFs of 25–50 improved model simulation of marine NO_x concentrations. However, EFs of 100 were required to adequately simulate HONO measurements in the remote marine boundary layer, resulting in an overestimate of NO_x relative to observations. Shah et al. (2023) successfully reproduced NO observations in the free troposphere when applying an EF of 100, scaled to the aerosol sea-salt: nitrate ratio, but did not evaluate the model's ability to reproduce HONO observations. Similarly Dang et al. (2023) used the same nitrate photolysis parameterization and again found

significant improvement in the modelling of NO_2 . These parameterizations were not based directly on the observed HONO mechanism but rather by reverse-engineering the process to produce the expected NO_x and O_3 concentrations. Thus, knowledge of the precise impact of nitrate photolysis as seen in laboratory and field studies and the effect of measured HONO on the wider atmospheric chemistry system is currently unknown.

Here we assume that this photolytic source of HONO from nitrate photolysis is the missing source required to reconcile HONO observations in environments with low NO_x concentrations. We use recent measurements of HONO made in remote locations (Sect. 2.1), together with the GEOS-Chem chemistry transport model (Sect. 2.2) to develop a new parameterization of the Enhancement Factor (EF) (Sect. 3) and implement it into the model. We then assess the impact of this parameterization on HONO concentrations (Sect. 4) and on the impact of nitrate photolysis on the composition of the troposphere (Sect. 5). The wider impacts of this process on our understanding of atmospheric chemistry are then discussed in Sect. 6.

2 Methods

Here we describe the datasets and tools used for the analysis. We first describe field observations of the concentration of HONO and other species and then the configuration of the GEOS-Chem model.

2.1 Field Measurements

2.1.1 ARNA Campaign

The ARNA (Atmospheric Reactive Nitrogen over the remote Atlantic) field campaigns took place over the tropical Atlantic Ocean in August 2019 and February 2020 using the FAAM BAe-146-301 atmospheric research aircraft and in August 2019 at the Cabo Verde Atmospheric Observatory (CVAO; Fig. S1 in the Supplement). Twelve flights (four in summer and eight in winter) were conducted with in situ measurements including NO, NO2, HONO, O3, and aerosol surface area. pNO_3^- was determined from aerosol filters sampled over each straight-and-level run. HONO concentrations were determined using differential photolysis as described in Andersen et al. (2023). This technique photolytically converts both NO₂ and HONO into NO. Subsequently, NO is detected using chemiluminescence with a dual-channel instrument featuring two custom-built photolytic converters. HONO conversion efficiencies were calibrated against measurements from ultraviolet-visible cavity enhanced absorption spectroscopy conducted at HIRAC (The Highly Instrumented Reactor for Atmospheric Chemistry), following the methodology of Reed et al. (2016). The average detection limit for HONO across the study period was 4.2 ppt at the 2σ level. At the CVAO, NO_x , pNO_3^- , O_3 , and photolysis rates

are measured routinely (Carpenter et al., 2010) and these were supplemented by HONO measurements described in Sect. 2.1.5.

2.1.2 FIREX-AQ

The FIREX-AQ campaign was conducted from July to September 2019, with multiple aircraft deployed from California, Idaho and Kansas in the USA (Bourgeois et al., 2022; Warneke et al., 2023). The datasets were collected from an archived merged dataset (https://www-air.larc.nasa.gov/cgi-bin/ArcView/firexaq, last access: 21 November 2025), averaged over 60 s intervals. In order to get measurements representative of "clean" or background air, measurements are excluded when the concurrent CO concentration exceeds 120 ppb, which would be indicative of pollution from either a biomass burning or anthropogenic source.

HONO was measured using an iodine-adduct chemical ionization mass spectrometer (CIMS) (Lee et al., 2014; Veres et al., 2020; Bourgeois et al., 2022). Ambient air mixed with reagent ions, specifically iodide ions and iodide-water clusters, was ionized and analyzed for mass-to-charge ratio. HONO was detected as a cluster with iodide, and background signals were accounted for to determine ambient HONO levels. The fixed-temperature measurement uncertainty is $\pm (15\% + 3 \text{ ppt})$, with a precision of $\pm 2 \text{ ppt}$ for 1 s data. NOx was measured with ozone induced chemiluminescence, with three channels measuring NO, NO₂ and NO_y, respectively. The instrument continuously samples ambient air from an aircraft, with specific flow rates for each gas. Instrument calibrations occur both on the ground and in-flight, and measurements are taken with high temporal resolution. Corrections are applied for factors like water vapor content and interference from other compounds. The estimated measurement uncertainties at 1hz for NO, NO₂, and NO_y at sea level are $\pm (4\% + 6 \text{ ppt})$, $\pm (7\% + 20 \text{ ppt})$, and $\pm (12\% + 15 \text{ ppt})$, respectively.

Carbon monoxide (CO) was measured by tunable diode laser absorption spectroscopy (TDLAS) using the DACOM (Differential Absorption Carbon monoxide Measurement) instrument (Sachse et al., 1987; Sachse Jr. et al., 1991; Bourgeois et al., 2022). TDLAS used three single-mode tunable diode lasers, measuring CO using a quantum cascade laser (QCL) at $4.7 \, \mu m$. Measurement precision (1σ), calculated after the campaign, was approximately $0.1 \, \%$ at $1 \, s$.

Bulk nitrate aerosol measurements used to produce the nitrate photolysis parameterization (Fig. 2) were made with the Soluble Acidic Gases and Aerosol (SAGA) filter collector with subsequent offline IC analysis (Dibb et al., 1999; Dibb et al., 2002; Scheuer et al., 2003). Sample resolution during FIREX-AQ was 2–5 min. Concentrations of chloride and other ions were also reported. SAGA has a detection limit of 1 to 25 ppt depending on the sampled species.

A high-resolution aerosol mass spectrometer (HR-AMS) was used to measure fine-mode particulate nitrate (pNO_3^-)

at a high time resolution (Guo et al., 2021; Bourgeois et al., 2022). Submicron aerosol composition was derived using flash vaporization of the aerosol, followed by $70\,\mathrm{eV}$ electron ionization of the volatilized gas phase and analysis by mass spectrometry. Typical detection limits were $\sim 30\,\mathrm{ppt}$.

2.1.3 CAFÉ-Africa

The Chemistry of the Atmosphere: Field Experiment in Africa (CAFE-Africa) campaign took place in August and September 2018, with 14 flights from Cabo Verde over the Atlantic Ocean and West African coastline. A "mini-DOAS" was deployed on the German High-Altitude and Long-Range (HALO) research aircraft to measure HONO. The mini-DOAS is an airborne six-channel optical spectrometer, which records UV, visible, and near infra-red light in the nadir and limb viewing geometries. The spectrometers are kept in an evacuated and cooled housing in the otherwise unpressured, uninsulated fuselage of the HALO aircraft. Collected skylight spectra are analysed for signatures of light absorption by trace gases using the DOAS technique. Slant column densities of trace gases determined by the DOAS technique are then converted to volume mixing ratios or concentrations by the novel scaling method. The scaling method requires a gas whose concentration is known or otherwise measured in situ, to construct a proportional relationship between concentrations and slant column densities. The Monte Carlo radiative transfer model McArtim helps to attribute absorption to specific layers of the atmosphere. Gas concentrations retrieved with the scaling method represent averages over several dozen square kilometres as a function of the mean light path length, as well as the distance travelled by the aircraft during integration of the spectra. Due to the dependence on pathlength and large variations with altitude and visibility, the limit of detection ranges from 1 ppt within the marine boundary layer (MBL) to 15 ppt near 15 km altitude.

2.1.4 SEANA

The Shipping Emissions in the Arctic and North Atlantic atmosphere (SEANA) project took place between 20 May and 26 June 2022 around the coast of Greenland (Zhang et al., 2024). HONO was measured using a Long Path Absorption Photometer (LOPAP-03, Quma GmbH) during the DY151 cruise aboard the RSS Discovery research ship. HONO was sampled within a stripping coil into an acidic solution and derivatized with an azo dye. Absorption of light (550 nm) by the azo dye was measured with an Ocean Optics spectrometer using an optical path length of 2.4 m. The technique is described in detail in Heland et al., 2001. The instrument was calibrated and operated following the standard operating procedures described in Kleffmann and Wiesen (2008).

The LOPAP instrument was located inside a shipping container on the foredeck of the ship and was sampling via a 3 m long umbilical to the inlet located on the roof of the ship-

ping container. The detection limit of the LOPAP during the cruise was between 0.7 and 1.5 ppt $(2\sigma, 30 \text{ s})$, with an estimated relative error of 10%.

A zero signal was taken at regular intervals (6 h) by overflowing the inlet with dry nitrogen for 30 min. The zero signals were linearly interpolated to obtain a baseline which was then subtracted from the calibrated signal. Because of the very low HONO levels in the Arctic Ocean, the LOPAP signal was sometimes indistinguishable from the zero signal. A correction factor of 1.5–3.5 ppt was therefore applied to the final time series on the assumption that the HONO concentration in the darkest period of the Arctic day is zero. Due to the inherent uncertainties in this assumption the reported values should be considered lower limits.

2.1.5 Cabo Verde Atmospheric Observatory

The Cabo Verde Atmospheric Observatory (CVAO) is a World Meteorological Organisation (WMO) Global Atmospheric Watch (GAW) site that operates on the north-west coast of São Vincente, Cabo Verde (16°51′ N, 24°52′ W). Measurements at the site are considered to be representative of clean, marine background air (Carpenter et al., 2010).

HONO has been measured at the CVAO in November-December 2015 (Reed et al., 2017), August 2019, February 2020 (Andersen et al., 2023) and in February 2023, using a long-path absorption photometer (LOPAP-03 QUMA Elektronik & Analytik GmbH). A full description of the instrument's operating principle and measurement technique can be found in Heland et al. (2001) and Kleffmann (2007). In the 2023 campaign, the inlet for the LOPAP was placed on top of a shipping container (roughly 3 m a.g.l.). Zeroes were measured every 6 h for 30 min using an N5 N₂ cylinder. The instrument was calibrated using a Titrisol nitrite standard solution (1000 mg of NO_2^- diluted to 0.01 mg L^{-1}) on 9, 11 and 21 February. The detection limit was 0.3 ppt (2 s), calculated using the noise during zero measurements. As recommended by QUMA, the relative error of the instrument was set at 10 % of the measured HONO value. Particulate nitrate (pNO_3^-) was measured in 24 h samples using a PM₁₀-inlet and subsequent laboratory analysis using standard ion chromatography technique (Fomba et al., 2014).

2.1.6 Tudor Hill Observatory

The Tudor Hill Marine Atmospheric Observatory is a continuous monitoring station located on the island of Bermuda (32°15′ N, 64°52′ W). In field studies in 2019, ambient HONO concentrations were measured continuously by a long-path absorption photometry (LOPAP) system (Zhu et al., 2022). Corrections were done using the zero-HONO air generated by pulling ambient air through the Na₂CO₃ denuder. The LOPAP system, described in detail in Zhu et al. (2022), has been widely used and proven accurate in HONO measurement during the previous NOMADSS field

campaigns (Ye et al., 2016, 2017). The detection limit was calculated as $\sim 0.6 \, \mathrm{ppt}$ at 10 min time resolution. Ambient HNO₃ and $p \, \mathrm{NO_3^-}$ were also measured by similar LOPAP systems, where the nitrate was converted into nitrite through a Cd column in NH₄Cl buffer solution. The detection limit of particulate nitrate measured by the LOPAP system was $\sim 17 \, \mathrm{ppt} \, (3\sigma)$ at 10 min time resolution. NO_x concentrations were measured by a low-level commercial chemiluminescence analyzer.

2.1.7 ATom

The NASA Atmospheric Tomography mission (ATom) consisted of four aircraft campaigns conducted between August 2016 and May 2018 (Wofsy et al., 2021; Thompson et al., 2022). Using NASA DC-8 research aircraft, ATom provided detailed datasets of atmospheric composition with an extensive spatial coverage, in particular over oceans. Here used the 10 s merged ATom dataset for all four seasonal campaigns (https://doi.org/10.3334/ORNLDAAC/1925) (Wofsy et al., 2021). The data was filtered to only use data measured over the ocean, to broadly avoid polluted air.

2.2 GEOS-Chem

The three simulations were completed using the 3-D global chemical transport model GEOS-Chem, version 14.2.2 (Bey et al., 2001) (http://www.geos-chem.org, last access: 31 March 2024; https://doi.org/10.5281/zenodo.12809895, The International GEOS-Chem User Community, 2024). The model was driven by MERRA-2 meteorology from the NASA Global Modeling and Assimilation Office (Gelaro et al., 2017), with 72 vertical levels and a spatial resolution of $4.0^{\circ} \times 5.0^{\circ}$. All simulations were run for 2 years through 2018 and 2019, with the first year considered spinup. The model used an updated chemical mechanism with improved benzene, toluene and xylene oxidation chemistry, as described by Bates et al. (2021). The model used biomass burning emissions from GFED4s (van der Werf et al., 2017) and biogenic emissions from MEGAN v2.1 (Guenther et al., 1995). Anthropogenic emissions are from the Community Emissions Data System (CEDS) (Hoesly et al., 2018; Mc-Duffie et al., 2020).

The Shah parameterization for nitrate photolysis was developed by Shah et al. (2023) and is incorporated into the standard GEOS-Chem model. They found best agreement with NO observation with an EF of 100 applied to coarse-mode nitrate, while the EF for fine-mode nitrate was scaled based on the pNO_3^- to sea-salt ratio. For the purposes of this study, nitrate photolysis according to Shah et al. (2023) was switched off in the model for the "Base" simulation and turned on in the "Shah" simulation.

When simulating the preindustrial atmosphere, anthropogenic emissions for the year 1750 are taken from CEDS (Hoesly et al., 2018), with natural emissions matching the

present-day simulations and meteorology for the year 2019. Methane (CH₄) for the year 1750 is prescribed from the CMIP6 dataset (Meinshausen et al., 2017). A normalised radiative forcing (NRF) of 42 mW m⁻² DU⁻¹ (Stevenson et al., 2013) is used to calculate the preindustrial to present-day O_3 radiative forcing.

Normalized mean bias is used to assess model performance compared to observations, defined here as

NMB =
$$\frac{\sum_{i=1}^{n} (P_i - O_i)}{\sum_{i=1}^{n} (O_i)}$$

where *P* are the simulated values and *O* is the observations. The nitrate photolysis parameterisation was developed by fitting a non-linear least squares function to the observed data, using the SciPy python package (https://docs.scipy.org/doc/scipy-1.15.0/reference/generated/scipy.optimize.curve_fit.html, last access: 23 November 2025; Virtanen et al., 2020).

3 Development of a nitrate aerosol photolysis parameterization

Here we use observations of HONO, nitrate aerosol and photolysis rates from (1) the Atmospheric Reactive Nitrogen over the remote Atlantic (ARNA) aircraft campaign over the Tropical Atlantic (Andersen et al., 2023), (2) the Fire Influence on Regional to Global Environments Experiment - Air Quality (FIREX-AQ) aircraft campaign over the continental USA (Warneke et al., 2023) and (3) HONO measurements from the Cabo Verde Atmospheric Observatory (see Methods Section), to generate a parameterization of the nitrate aerosol photolysis process. This is then applied in GEOS-Chem to simulate HONO concentrations and evaluated with independent HONO measurements from the Chemistry of the Atmosphere: Field Experiment in Africa (CAFE-Africa) aircraft campaign in the Atlantic (Weyland, 2024), the Shipping Emissions in the Arctic and North Atlantic Atmosphere (SEANA) ship campaign and from Tudor Hill, Bermuda (Zhu et al., 2022). The locations and measured concentrations of HONO in the various campaigns are shown in Fig. S1 in the Supplement.

Following Ye et al. (2016), we assume that the photolysis of nitrate aerosol leads to the production of 0.66 HONO molecules and $0.33~\text{NO}_2$ molecules (Reaction R1). The photolysis of HONO is its dominant sink (Reaction R2) with a lifetime in the tropical marine boundary layer of about 12 min during the day (Ye et al., 2016; Andersen et al., 2023) and thus we derive a rate equation by placing HONO into steady state (Eqs. 1 and 2).

$$HONO + h\nu \rightarrow OH + NOJ_{HONO}$$
 (R2)

Thus;

$$\frac{d[\text{HONO}]}{dt} = \frac{2}{3} \times J_{pNO_3^-} [pNO_3^-] - J_{\text{HONO}} \times [\text{HONO}] \quad (1)$$

$$[\text{HONO}] = \frac{2}{3} \times \frac{J_{pNO_3^-}}{J_{\text{HONO}}} \times [pNO_3^-] \quad (2)$$

Where $J_{\rm HONO}$ and $J_{\rm NO_3^-}$ refer to the rate of photolysis of HONO and $p{\rm NO_3^-}$, respectively. Following Ye et al. (2016) we assume that the photolysis of nitrate is equal to the photolysis rate for gas phase HNO₃ ($J_{\rm HNO_3}$) multiplied by an enhancement factor (EF) which can be rearranged to give Eq. (3).

$$EF = \frac{3}{2} \times \frac{[\text{HONO}]}{[p\text{NO}_3^-]} \times \frac{J_{\text{HONO}}}{J_{\text{HNO}_3}}$$
 (3)

The renoxification process is thought to be efficiently driven by photolysis of surface-bound rather than bulk nitrate or nitric acid, due to enhanced absorption cross sections and higher quantum yields at the interface compared to bulk solution (Zhu et al., 2010; Du and Zhu, 2011; Ye et al., 2017). Further, the presence of certain cations has been shown to lead to preferential distributions of nitrate ion at the interface (Wingen et al., 2008; Richards and Finlayson-Pitts, 2012; Hua et al., 2014). Therefore, following Andersen et al. (2023), we fit a nonlinear function to the observed EF (see Methods Section), derived from the measurements of HONO, nitrate aerosol, $J_{\rm HNO_3}$ and $J_{\rm HONO}$ from the CVAO, ARNA and FIREX-AQ campaigns, to a Langmuir isotherm model (Eq. 4, Fig. 1).

$$EF = \frac{5.02 \times 10^8}{1 + 7.19 \times 10^5 \times [pNO_3^-]}$$
 (4)

We note though that unlike the fit in Andersen et al. (2023), the Eq. (4) no longer resembles a Langmuir isotherm as the nitrate-dependent portion of the denominator under realistic atmospheric conditions is significantly larger than 1. The differences between the parameterizations may reflect the mixed contribution of surface and bulk processes, and the different aerosol compositions in the different field campaigns used (see discussion below). In the limit of large nitrate concentrations, the new EF tends towards $700/|pNO_3^-|$, whereas the Andersen et al., parameterization tends to a value of $2040/[pNO_3^-]$. In this limit, HONO production from nitrate photolysis $(J_{HNO_3} \times EF \times [pNO_3^-])$ becomes independent of the nitrate concentration for both parameterizations. Whereas the Andersen et al. (2023), formula reached this limit at concentrations of nitrate around $5 \,\mathrm{nmol}\,\mathrm{m}^{-3}$, the new function reaches this at much low values of nitrate $(\sim 1 \times 10^{-6} \, \text{nmol m}^{-3})$. However, given the concentrations of nitrate seen in the atmosphere, most of the troposphere will be in this nitrate independent regime for both parameterizations.

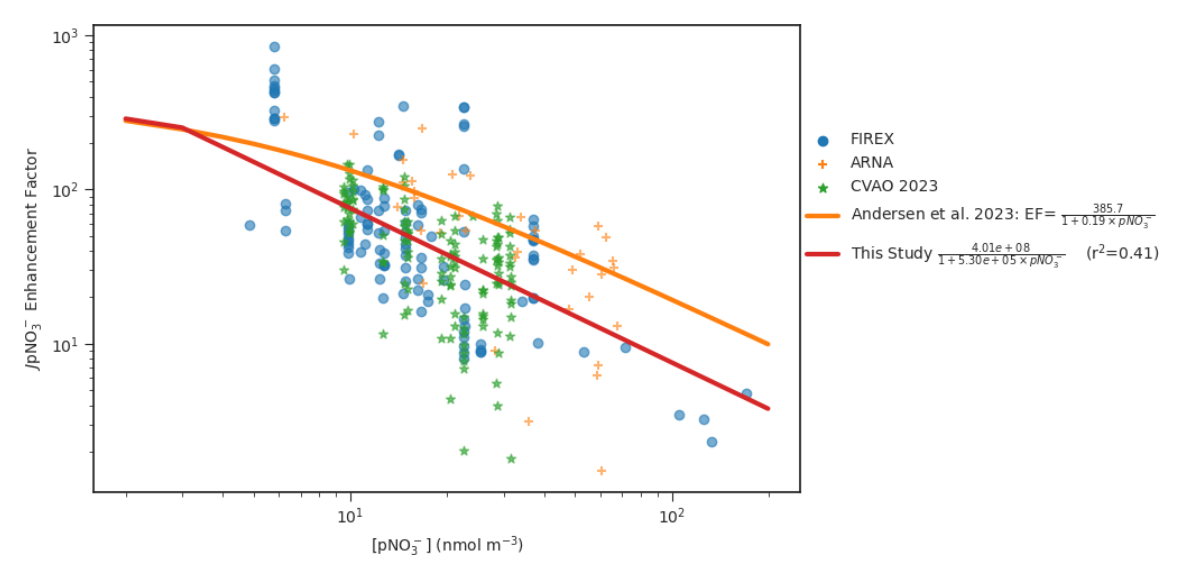


Figure 1. Nitrate aerosol photolysis enhancement factor necessary to balance the observed HONO against its photolytic loss as a function of the nitrate aerosol concentration (see Methods Section).

The large range in the estimated EFs from measurements (Fig. 1) results in large variance around the fit, with an Rsquared value of 0.41. For a particular nitrate concentration there is an order of magnitude variation in the calculated EF. This is not surprising since the measurements span a variety of environments, likely experiencing different aerosol pH, composition (notably Cl⁻ and Br⁻ concentrations) and ambient humidity, all of which are known to impact the efficiency of renoxification (Ndour et al., 2009; Gen et al., 2022; Andersen et al., 2023; Sommariva et al., 2023; Li et al., 2024; Jiang et al., 2023) However, more complex parameterizations accounting for such dependencies resulted in only minor improvements in the agreement with observed EFs (see examples in Fig. S2 in the supplementary material). Therefore, for the sake of simplicity and due to the paucity of observations, the parameterization with only pNO_3^- dependency was used here. Future work both in the laboratory and the field will be required to better constrain the functional form of EF under an appropriate range of ambient conditions.

The mean EF values calculated from the combined ARNA, FIREX-AQ and CVAO measurements are 2–3 times lower than that found in Andersen et al. (2023) using the ARNA campaign alone. This may reflect that the FIREX-AQ observations were over a continental region whereas the Andersen data was collected over the ocean, where sea salt aerosol dominates the aerosol mass. Sodium and chloride ions have been observed to enhance the yield of HONO and NO₂ from particulate nitrate photolysis, attributed to the existence of a double layer of interfacial Cl⁻ and subsurface Na⁺ drawing nitrate ions closer to the interface when the Cl⁻: NO₃⁻ ratio increases (Wingen et al., 2008; Sommariva et al., 2023). The observed bulk chlorine from filter measurements during the ARNA campaign was substantially higher than dur-

ing FIREX-AQ (median value of $0.63\,\mu g\,m^{-3}$ compared to $0.03\,\mu g\,m^{-3}$), reflecting the contrast between marine and terrestrial campaigns and possibly contributing to the difference in calculated EF.

Our parameterization produces a much greater range of EF values (from 3 to 562) than used in previous nitrate photolysis modeling studies (Kasibhatla et al., 2018; Shah et al., 2023). Kasibhatla et al. (2018) used fixed EF values (of between 25–100) on sea-salt aerosol and Shah et al. (2023) tied the EF magnitude to the availability of sea-salt with fixed upper and lower EFs, resulting in a range of 10 to 100. While these studies demonstrated that nitrate photolysis could improve model performance in simulating NO_x and O_3 , the resulting parameterizations were not based on the EF values derived in laboratory and field studies (Ye et al., 2016; Shi et al., 2021).

4 Evaluation of parameterisation

Here we implement the parameterization of the enhancement factor (Eq. 1) into the GEOS-Chem model (see Methods Section and Eq. 4). We evaluate this model simulation together with a version with no nitrate photolysis (Base) and that using the Shah et al. (2023) parameterization (Shah) against a wider set of pNO_3^- (Prospero, 1999; Prospero and Lamb, 2003; Savoie et al., 2002) and HONO observations (CAFE-Africa, SEANA, Tudor Hill). We use a normalized mean bias (NMB; see Methods Section) metric to assess model performance and impact of changes between simulations.

The extent and impact of the simulated nitrate photolysis relies critically on the model's ability to replicate nitrate aerosol. Nitrate aerosol in GEOS-Chem is split into two modes; a fine-mode associated with sulfate and ammonia

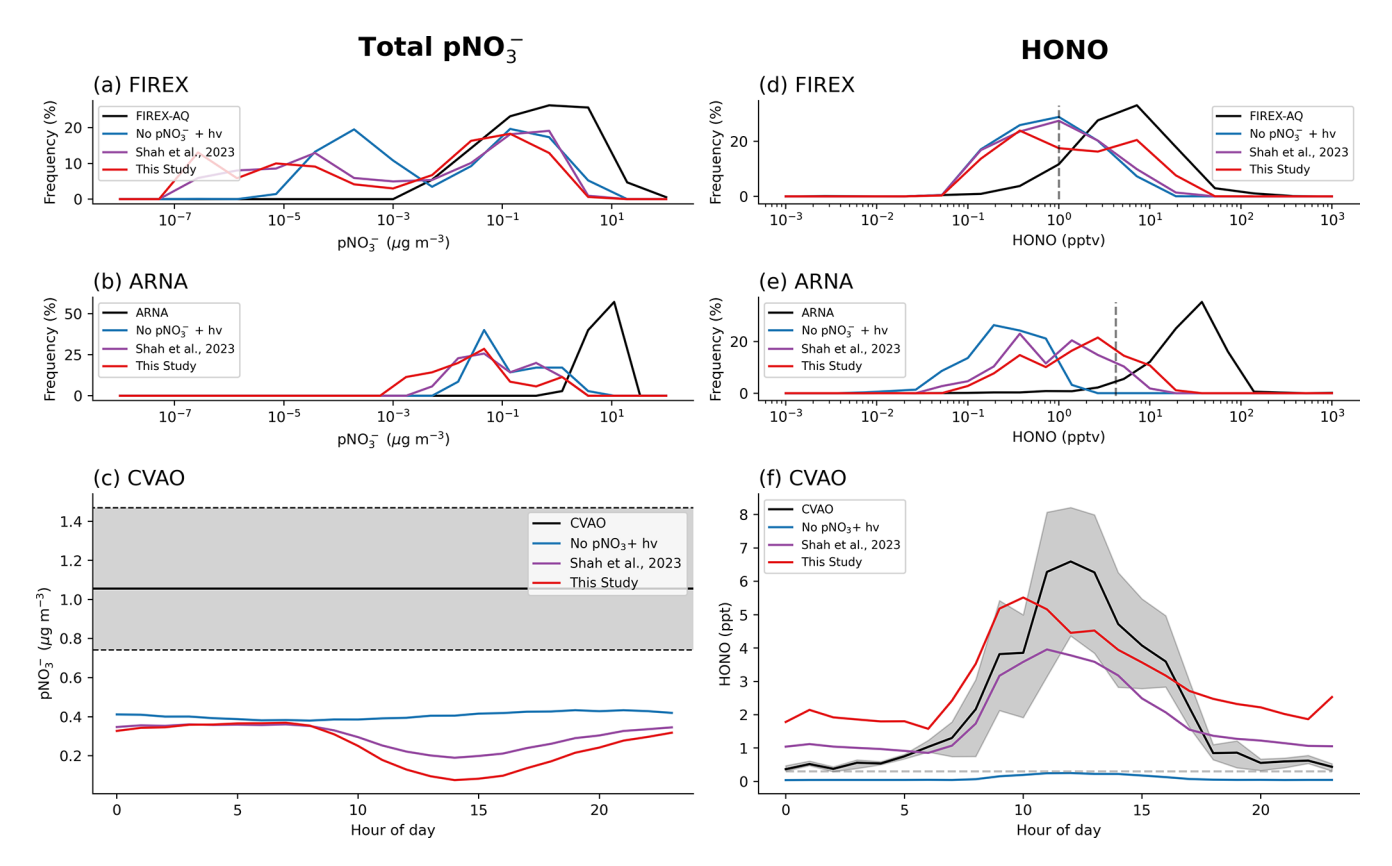
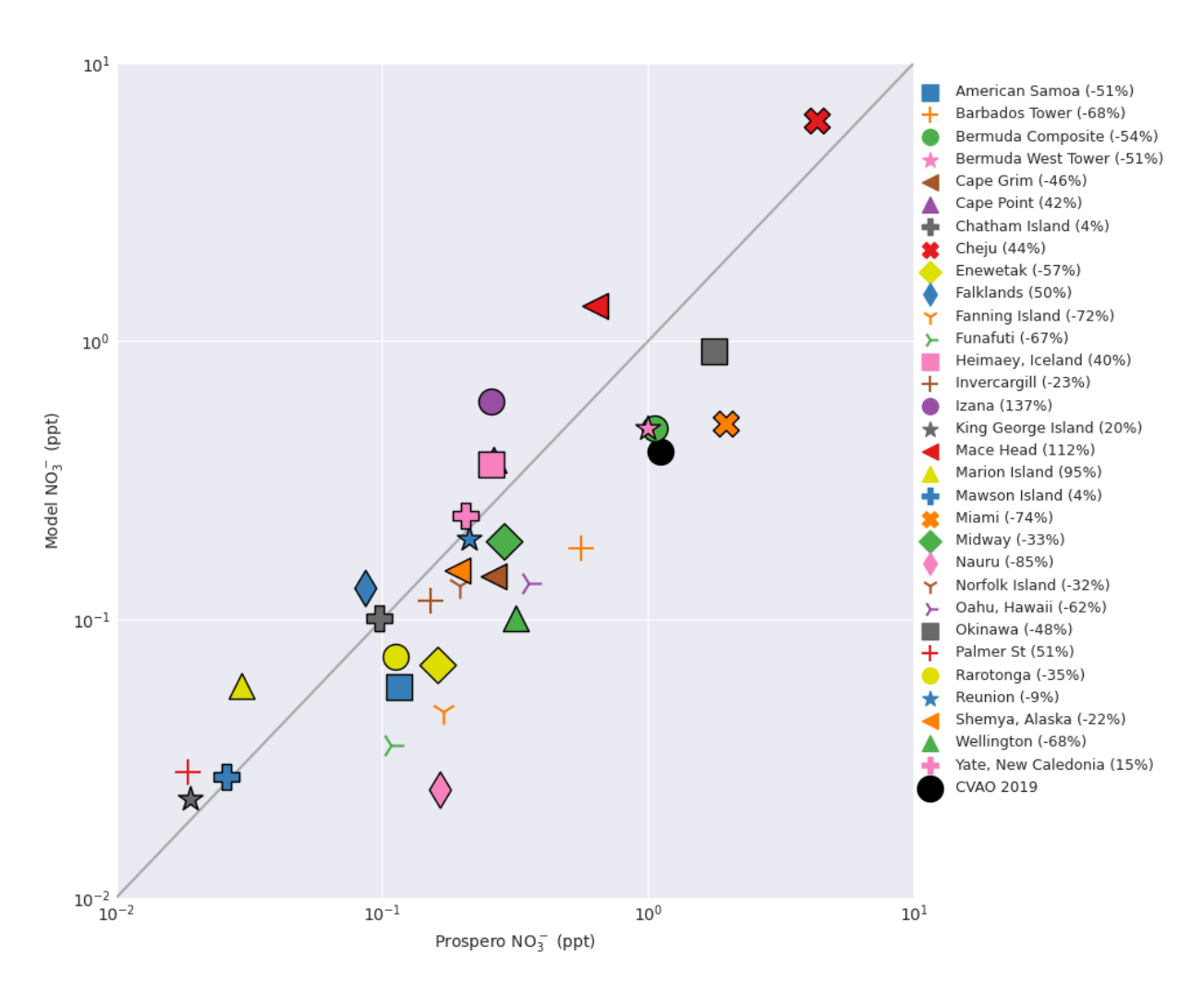


Figure 2. Frequency density comparisons between observed (black) and simulated (Base simulation (blue); Shah simulation (purple); New parameterization (red)) total (coarse and fine mode) pNO_3^- (left) and HONO (right) concentrations during the FIREX-AQ campaign (top) and the ARNA campaign (middle). Bottom panels show simulated diurnal concentrations over the Cabo Verde Atmospheric Observatory (CVAO) compared to available observations (HONO diurnal averaged from campaigns in 2015, 2019 and 2023 represented by the black line, grey shading indicating 10th–90th percentile in panel $\bf c$, 25th-75th percentile in panel $\bf f$). Dashed grey lines in panels ($\bf d$), ($\bf e$) and ($\bf f$) represent the estimated limit of detection.

and a coarse-mode (0.5–8.0 µm) associated with sea-salt and desert dust. Various studies have reported a persistent highbias in fine-mode nitrate aerosol in GEOS-Chem compared to aerosol mass spectrometry (AMS) observations (Walker et al., 2012; Miao et al., 2020; Zhai et al., 2021a, b; Gao et al., 2022). This may be linked to the model underestimating acidity in remote regions (Nault et al., 2021). There has been little work evaluating the coarse-mode nitrate. Consistent with previous studies, we find that the base simulation without nitrate photolysis significantly overestimates fine-mode nitrate when compared with observations from the NASA Atmospheric Tomography Mission (ATom) campaign (Fig. 6a, NMB = +271 %) and in some regions of the mid and upper troposphere in the FIREX-AQ campaign (Fig. 6), except over California where nitrate is very low, likely due to an underestimate of ammonia emissions (Walker et al., 2012). The inclusion of the nitrate photolysis parameterization generally decreases fine nitrate aerosol concentrations and improves the NMB relative to observations for the ATom campaign from +271 % to +93 % (Fig. 6a).

In contrast, total particulate nitrate (coarse and fine) (Fig. 2a-c) observations from FIREX-AQ, ARNA, and CVAO are underestimated by the base model with a NMB of -88% to -95%. The inclusion of nitrate photolysis has only a small impact, decreasing aerosol concentrations and resulting in a NMB of between -92% and -98% across the 3 datasets. A further comparison with global surface observations collected between 1980 and the present (the Prospero network, Fig. 3), also shows the model underestimates total nitrate at the majority of sites. This is likely to be of larger importance in regions with a higher ratio of coarse to fine mode aerosol, such as marine regions where coarse sea-salt aerosol is prominent. Overall, we conclude, consistent with previous studies (Walker et al., 2012; Miao et al., 2020; Zhai et al., 2021a, b; Gao et al., 2022), that the model overestimates fine mode nitrate and significantly underestimates coarse mode. Inclusion of nitrate photolysis improves the comparison with fine mode nitrate and leads to a distinct diurnal profile in pNO₃ which decreases around midday and steadily increases overnight (Fig. 2c). As sea salt nitrate makes up > 90 % of the nitrate at Cabo Verde in the



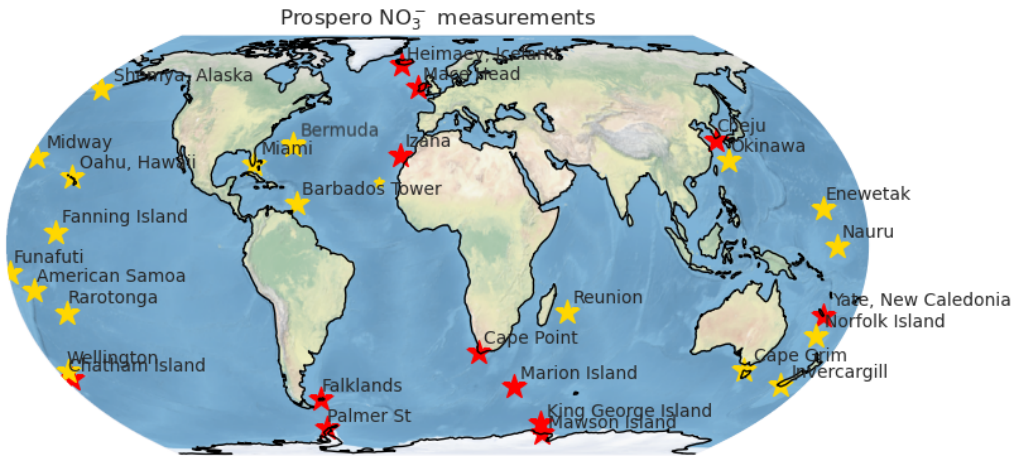


Figure 3. Comparison of total nitrate (pNO_3^-) measurements from the Prospero network (Prospero, 1999; Prospero and Lamb, 2003; Savoie et al., 2002) with simulated nitrate in the base model simulation. Lower panel shows the locations of the sites. Colour of the marker on the map indicates whether the model overestimates (red star) or underestimates (yellow) observations.

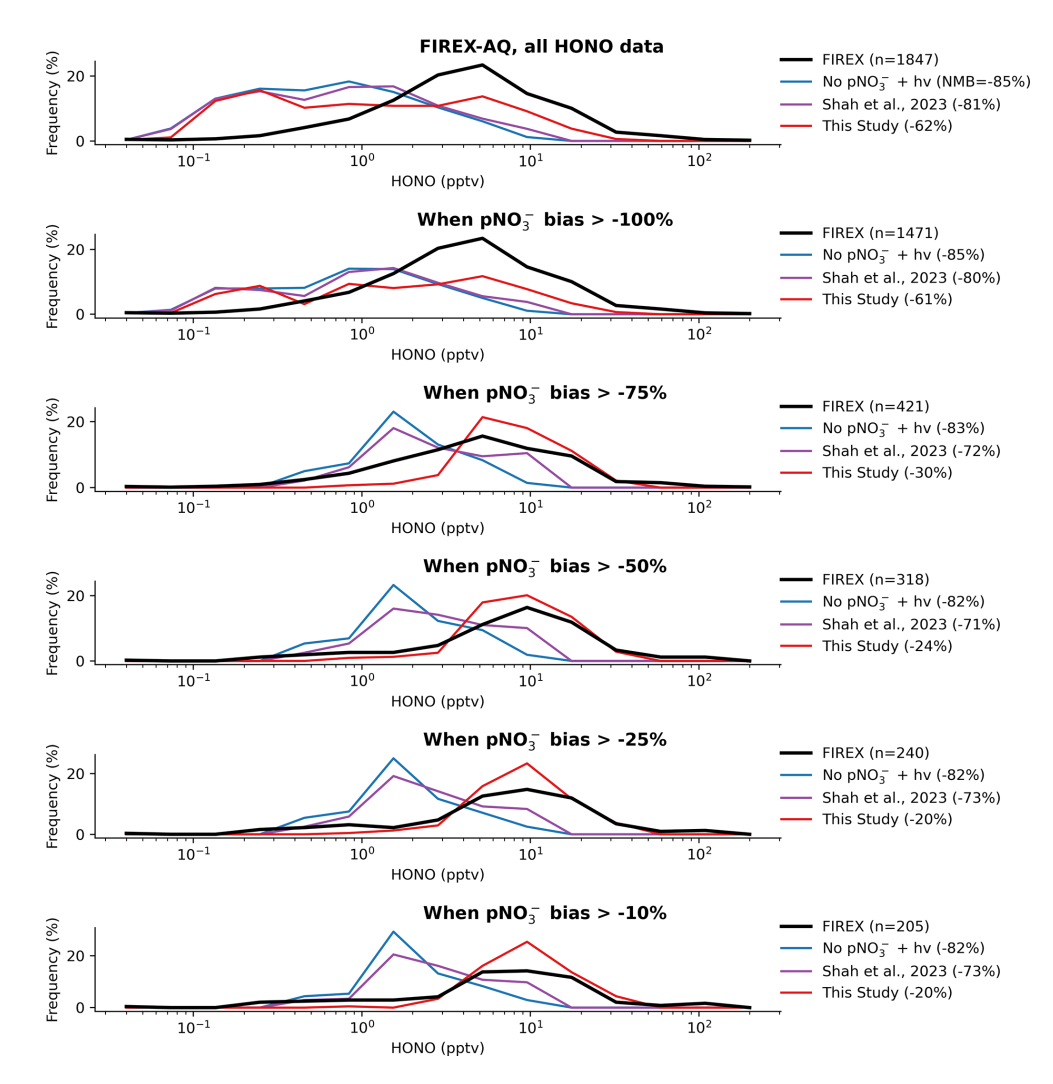


Figure 4. HONO from the FIREX-AQ campaign (black line) compared with simulated HONO for all data (top panel) and with the data filtered by various degrees of pNO_3^- error (lower panels). Number of data points after filtering is shown in the legend of each panel, as well as the NMB of each model simulation.

model, mostly in the coarse mode, the pNO_3^- diurnal simulated here is a result of photolysis depleting nitrate aerosol. There appear to be no marine coarse mode nitrate observations at a high enough time resolution available to evaluate this result. Improvement in the performance of the model for coarse mode marine nitrate is clearly a key step for progress it to be made in assessing the importance for nitrate photolysis in the marine environment.

Figure 2d–f compares the simulations of HONO "background" air (selected as described in Methods Section) with observations from FIREX-AQ, ARNA and the CVAO. Observed HONO mixing ratios across the 3 datasets range between 1 to 100 ppt. Without nitrate photolysis, simulated mixing ratios are substantially lower (<1 ppt) than observations. The inclusion of the Shah parameterization decreases the bias by increasing HONO concentrations at the CVAO (NMB improves from -95% to -16%), with only minor

changes for the airborne ARNA (-97% to -95%) and FIREX-AQ (-92% to -81%) campaigns. Inclusion of the new nitrate parameterization increases peak daytime HONO concentrations to >4 ppt for all campaigns, in better agreement with observations. It does however lead to a mean nighttime overestimate of 1.5 ppt (Fig. 2f). This is potentially due to dry deposition of HONO in the model being too slow, resulting in higher overnight concentrations than in observations (Yu et al., 2022).

While the inclusion of nitrate photolysis increases HONO concentrations, there remains a daytime underestimate of HONO relative to each of these datasets. This is likely due to the model being biased low for total nitrate concentrations, and thus the model HONO production being too low. To test this hypothesis, we further evaluated the HONO in the FIREX-AQ dataset, subsampling the entire dataset when the model shows various degrees of underestimate in pNO_3^-

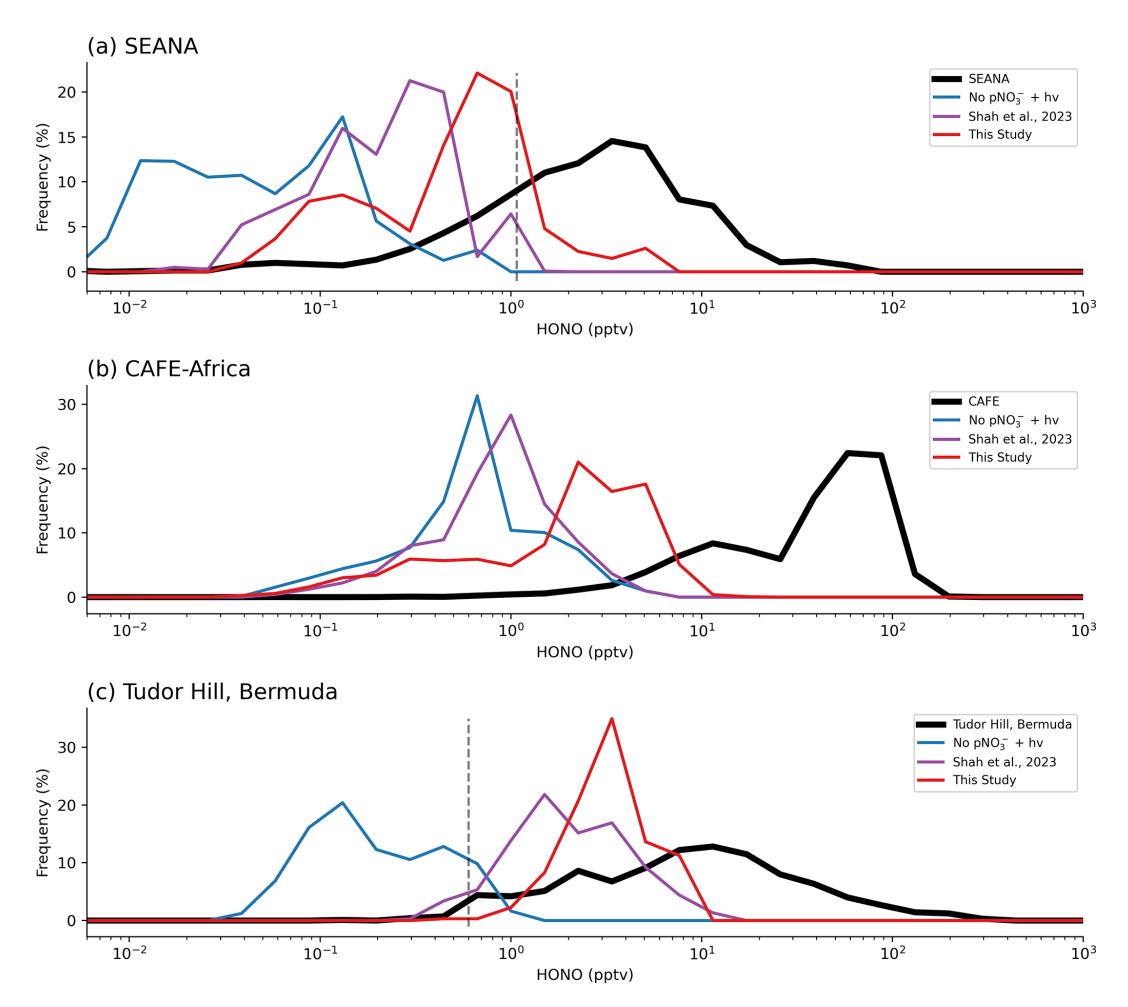


Figure 5. Frequency density comparisons between observed and simulated HONO concentrations during the (a) SEANA ship campaign (surface), (b) CAFE-Africa aircraft campaign and (c) in-situ measurements from Tudor Hill, Bermuda (surface) (Zhu et al., 2022). Dashed grey lines represent the estimated limit of detection.

(Fig. 4). When sampling the entire FIREX-AQ dataset, the new parameterization reduced the model HONO underestimate by around a quarter (-85% to -62%). When ignoring data points where the simultaneous pNO_3^- measurement had a low bias of > 75 %, the HONO bias of the new simulation improved to -30%, while the bias in the Base and Shah simulations showed only very minor changes. The best agreement (NMB of -20%) was found with the new parameterization when only considering data with a pNO_3^- underestimate of less than 25 %. This demonstrates that the new parameterization is capable of reproducing measured HONO concentrations reasonably accurately when modelled $pNO_2^$ is close to observations and that the main limiting factor for the model simulation of HONO is the pNO_3^- bias. It was not possible to replicate this analysis for the ARNA and CVAO datasets due to the amount of data available.

The modelled HONO is also compared to measurements from independent datasets SEANA (ship), CAFE (aircraft) and Tudor Hill (in-situ) (see Methods Section) (Fig. 5).

Across all three datasets the base model has a large underestimate (-89%), which is somewhat reduced by the Shah parameterization (-84%) with further improvement from the new parameterization (-78%), but there remains a large low model bias for HONO. The comparison between the model and the CAFE-Africa campaign is very consistent with the ARNA comparison shown in Fig. 2, as these campaigns took place in a similar area of the Atlantic Ocean. Importantly, Figs. 2 and 5 demonstrate the persistence of marine background HONO, and highlight the model failure to reproduce these observations without nitrate photolysis or with previous parameterizations. The introduction of a rapid nitrate photolysis parameterization leads to improvements in the simulation, however the model and measurements of HONO cannot be reconciled without substantial improvement in the simulation of total nitrate aerosol in the model (as demonstrated in Fig. 4).

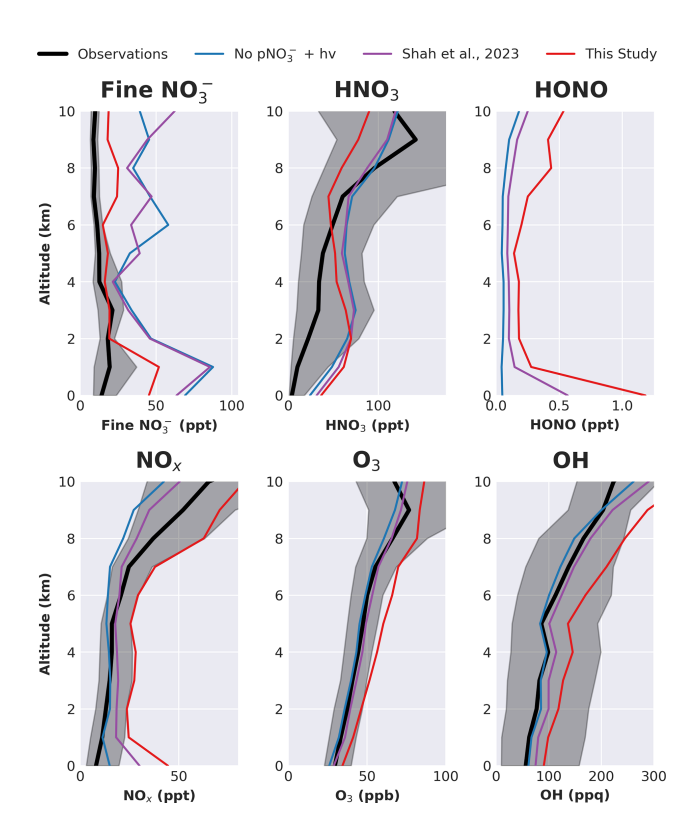


Figure 6. Median vertical profiles of key species from the ATom campaign (black, shaded area shows 25th–75th percentiles) and in GEOS-Chem simulations co-located with the measurements. Note: in contrast to Fig. 2, only fine mode nitrate, not the total, is compared here.

5 Impact on key atmospheric species

The model simulations with and without nitrate photolysis are compared to observed mean vertical profiles from the four NASA ATom missions in Fig. 6 (Wofsy et al., 2021). Without nitrate aerosol photolysis, fine mode nitrate aerosol is substantially overestimated by the model (NMB = 271 %), consistent with Gao et al. (2022). Introducing nitrate photolysis at the rate suggested by Shah et al. (2023) does not substantially change the model fine mode nitrate simulation (NMB = 243 %). However, introducing nitrate photolysis at the rate determined by Eq. (1) decreases fine mode nitrate, bringing it into better agreement with the observations (NMB = 93 %), particularly at 2–7 km (NMB = 20 %). The absence of a rapid nitrate photolysis parameterization may thus in part explain the persistent overestimate in fine-mode nitrate described by previous studies (Walker et al., 2012; Miao et al., 2020; Zhai et al., 2021a, b; Gao et al., 2022).

All three simulations overestimate the measured HNO_3 from the surface up to 6 km, before largely underestimating above 7 km. Observed values are just 4 ppt at the surface, compared with 24 ppt in the base simulation, 32 ppt with Shah and 37 ppt with the new parameterization. Throughout the ATom profile the base simulation had the lowest NMB

of 137 %, while the Shah run had the largest at 161 %. The new simulation had a NMB of 158 %, closer to the measured values in the mid-troposphere than the other simulations (5–7 km, NMB = 3 %), but with a larger underestimate in the upper troposphere (NMB = 33 %).

HONO measurements were not made during ATom. Without nitrate photolysis, modeled HONO concentrations are very low (< 0.1 ppt). The Shah parameterization increases concentrations roughly 10-fold in the marine boundary layer with surface concentrations reaching 0.5 ppt. Smaller increases are produced in the free troposphere (50 %–100 %). The new parameterization results in larger increases at the surface (20-fold increase) and has a larger impact through the free troposphere (2–5-fold increase). As a result, the average surface concentrations of HONO are generally > 1 ppt, above the typical instrument detection limit. Future measurements of HONO from airborne campaigns able to span a wide geographic range throughout the marine troposphere would be invaluable to further constrain the current uncertainties.

Without nitrate photolysis, the simulated NO_x is higher than observations at the surface (15 ppt vs 8 ppt measured), roughly consistent with the observations in the boundary layer and lower troposphere (NMB below 6 km = 3%), and lower than observations in the free troposphere (NMB above 6 km = 35%). The Shah parameterization, which was specifically derived to improve the model agreement with NO from ATom, unsurprisingly leads to good agreement throughout the profile (NMB = 7%), albeit with an overestimate at the surface (30 ppt). The new parameterization leads to a large overestimate at the surface (45 ppt) and throughout the vertical profile, more than doubling concentrations (NMB = 108%) and pushing concentrations beyond the observational variability.

 O_3 and OH concentrations during ATom are relatively well simulated in both the base and Shah simulations. Using the new parameterization leads to a large increase in both O_3 and OH (30 % and 53 %, respectively), again bringing their concentrations higher than the upper limits of observations.

6 Global Atmospheric Impacts

The tropospheric OH annual mean is $1.11 \times 10^6 \, \text{molec. cm}^{-3}$ in the base simulation, well within the range indicated by previous modeling studies of 0.94-1.44 (Zhao et al., 2019; Saunois et al., 2020), but higher than the 1.00×10^6 molec. cm⁻³ indicated by recent studies based on methyl chloroform observations (Zhao et al., 2023). Mean simulated tropospheric OH concentrations increase to 1.23 and 1.41×10^6 molec. cm⁻³ in the Shah and new parameterization simulations, respectively (Table 1). The model OH is at the upper limit of the range from previous studies with the faster parameterization, and substantially higher than the values suggested by observations. The NH:SH OH ratio (Table 2) is overestimated by all three

Table 1. Summary of key model diagnostics in the 3 GEOS-Chem simulations (percentage change from first simulation is in brackets).

Tropospheric	No $pNO_3^- + hv$	Shah et al. (2023)	This study
OH (× 10^6 molec. cm ⁻³)	1.11	1.23 (+11 %)	1.41 (+27 %)
CH ₄ lifetime (years)	9.65	8.54 (-12 %)	7.50 (-22 %)
NO_X burden (Tg)	0.36	0.40 (+11 %)	0.52 (+44 %)
CO burden (Tg)	326	306 (-6 %)	271 (-17%)
O ₃ burden (Tg)	319	342 (+7 %)	393 (+23 %)
O_3 radiative forcing (W m ⁻²)	0.43	0.49 (+14 %)	0.69 (+60 %)

Table 2. Annual mean tropospheric OH in GEOS-Chem simulations and previous literature, globally and for the ATom campaign (2016–2018).

	ОН			
	Global	NH	SH	NH/SH
ATom (× 10–4 ppq)				
Observations	1.8	2.1	1.4	1.48
No $pNO_3^- + hv$	1.5	2.1	1.3	1.61
Shah et al. (2023)	1.7	2.4	1.4	1.72
This study	3.4	3.3	1.6	2.05
Global (× 10^6 molec. cm ⁻³)				
Observations ^{1,2}	0.93-1.12			0.97 ± 0.12
Modelling studies ^{3,4}	0.93 - 1.44			
No $pNO_3^- + h\nu$	1.11	1.23	0.99	1.24
Shah et al. (2023)	1.23	1.38	1.07	1.29
This study	1.41	1.65	1.18	1.40

¹Patra et al. (2014); ² Cressot et al. (2014); ³ Naik et al. (2013); ⁴Zhao et al. (2023).

simulations during the ATom campaign, with the overestimate increasing with the introduction of nitrate photolysis and the associated increase in OH concentration. On a global scale, the model still overestimates the NH:SH ratio relative to observational estimates (Bousquet et al., 2005; Patra et al., 2014), although there remains large uncertainty on such estimates (Murray et al., 2013), but is in reasonable agreement with similar modeling studies (Zhao et al., 2023). Nitrate concentrations are higher in the NH primarily due to the distribution of anthropogenic emissions, meaning that the modeled impact of nitrate photolysis is also greater in the NH. As a result, the introduction of nitrate photolysis to the model exacerbates the existing overestimation in NH [OH], pushing the NH:SH ratio further from parity to 1.40 in our parameterization.

Figure 7 shows the impact of the new parameterization on global annual mean surface concentrations of HONO, NO_x and O_3 . Figure 8 shows the equivalent zonal mean plots. Surface HONO concentrations increase globally when the new nitrate photolysis parameterization is switched on, with maximum increases in mean surface concentrations of \sim 4–6 ppt found over Asia. Absolute increases are generally higher in the populated NH areas and relative changes are larger over

clean regions such as the Southern Ocean and tropical Atlantic/Pacific. Figure 9 shows the same as Fig. 7 but for HNO_3 , pNO_3^- and OH. As expected, surface pNO_3^- broadly decreases in remote regions, while HNO_3 and OH increase substantially.

For NO_x , the changes vary considerably between continental and ocean regions. The largest absolute changes are in industrialized, polluted regions (Eastern China, Eastern USA, Europe), where surface NO_x decreases by up to 1 ppb ($\sim 20\%$), due to an increase in the NO_2 to NO ratio as a result of the increased O_3 concentrations. This leads to a decrease in the lifetime of NO_x leading to decreased surface concentrations. Over the marine surface, NO_x increases by a factor of 2–4, particularly in the southern hemisphere. Polluted regions already have high levels of NO_x , meaning that the added NO_x from renoxification is relatively less important than in clean, low- NO_x environments. High NO_x concentrations also result in loss of O_3 through titration, limiting the impact in polluted areas (Monks et al., 2015).

The change in surface O_3 is more spatially homogeneous due to its longer lifetime. Relative to the simulation without nitrate photolysis, our parameterization increases annual mean global surface O_3 concentrations by 66%. By com-

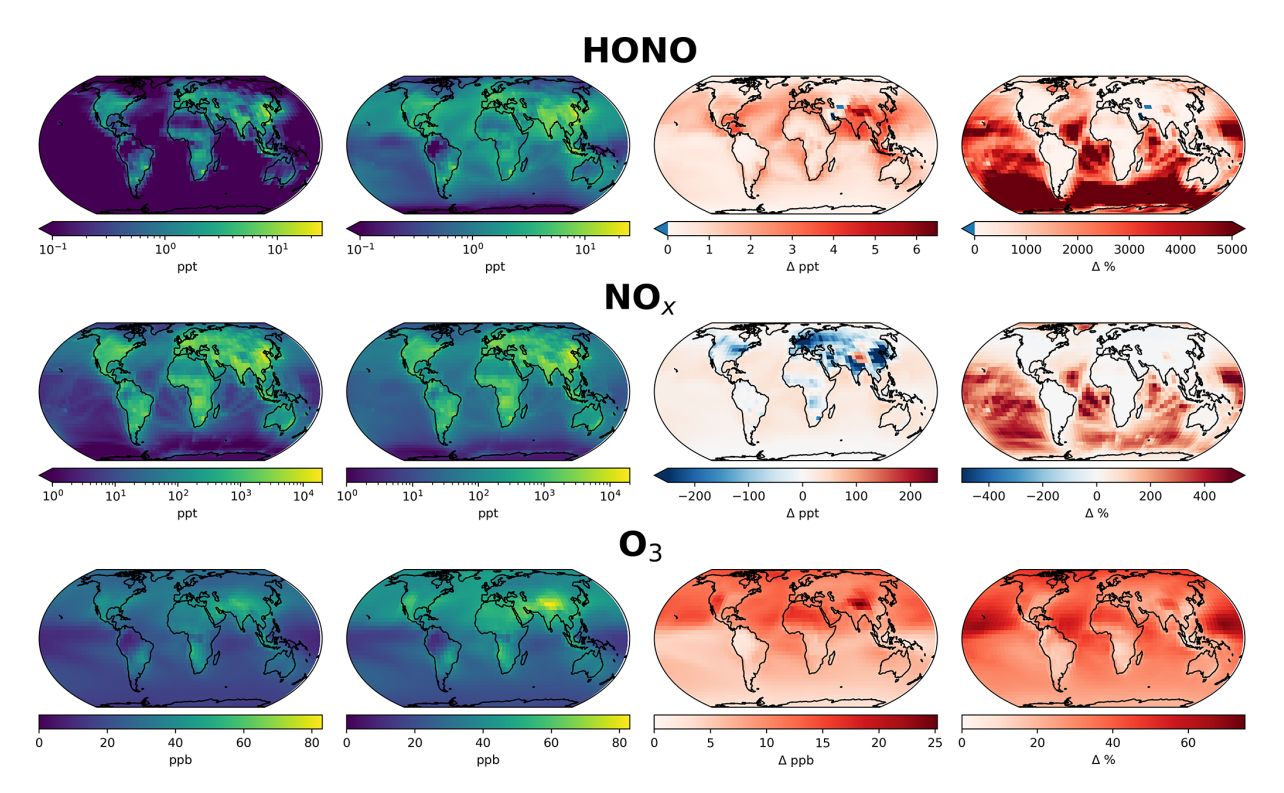


Figure 7. Annual mean surface concentrations of HONO, NO_x (NO+NO₂) and O_3 in model simulations (first column) without nitrate photolysis and (second column) with nitrate photolysis as parameterized by Eq. (1). Absolute difference is shown in the third column and % change in the fourth column.

parison, the Shah parameterization increases surface O₃ by 33 %. The largest changes are in the NH due to the greater concentration of nitrate. The troposphere in general is NO_x limited for O₃ production (Sillman and He, 2002; Ivatt et al., 2022), therefore the recycling of reactive nitrogen through nitrate photolysis leads to a near-ubiquitous increase in O₃ production. The greatest absolute increases of ~ 20 ppb are over NH continental regions and the highest relative increases occur over the tropical and subtropical oceans, where surface O₃ increases by up to 75 %, reaching close to 40 ppb in the mid-Pacific. Ozone mixing ratios over the tropical Pacific increase by up to 12 ppb (67 %). In populated and polluted regions, the changes tend to be significantly smaller, with increases of \sim 6 ppb (14%) and 9 ppb (20%) over Eastern China and Western Europe, respectively. A further comparison of O₃ with data from GAW sites (Fig. S3) demonstrates the large increase in O₃ in the simulation with the new parameterization, leading to a model overestimate at almost all sites. These analyses demonstrate that while the new parameterization may improve model performance for fine-mode nitrate aerosol and HONO relative to observations, it leads to a substantial inconsistency with observations of NO_x , O_3 and OH.

7 Discussion

The large increase in O_3 following the implementation of our new parameterization has a significant effect on the preindustrial (PI) to present day (PD) tropospheric O_3 radiative forcing (RF) (see Methods section and Table 1). The RF due to O_3 in both the base simulation and that using Shah et al. (2024)'s parameterization falls within the expected range from previous modelling studies (0.2–0.6 W m⁻², Myhre et al., 2013), with a 14% increase in RF in the Shah simulation. When using the new parameterization introduced here, the RF due to O_3 increases 60% from the base model to 0.69 W m⁻², outside of the range from previous modelling studies. There are large uncertainties associated with the nitrate aerosol in the preindustrial era, for which there is a lack of solid evidence to evaluate the preindustrial concentrations.

The new parameterization of nitrate photolysis developed here causes substantial changes in the chemical budgets of reactive nitrogen. NO_x is emitted into the atmosphere by anthropogenic combustion processes, biomass burning, lightning and soils, with a total source estimated at $\sim 55 \, \mathrm{TgN} \, \mathrm{yr}^{-1}$ dominated by anthropogenic combustion of $\sim 31 \, \mathrm{TgN} \, \mathrm{yr}^{-1}$ (Hoesly et al., 2018; McDuffie et al., 2020; Bray et al., 2021). Table S1 summarises the key terms. The most important change in the budget caused by fast nitrate photolysis is the recycling of nitrogen from stable species (pNO_3^-)

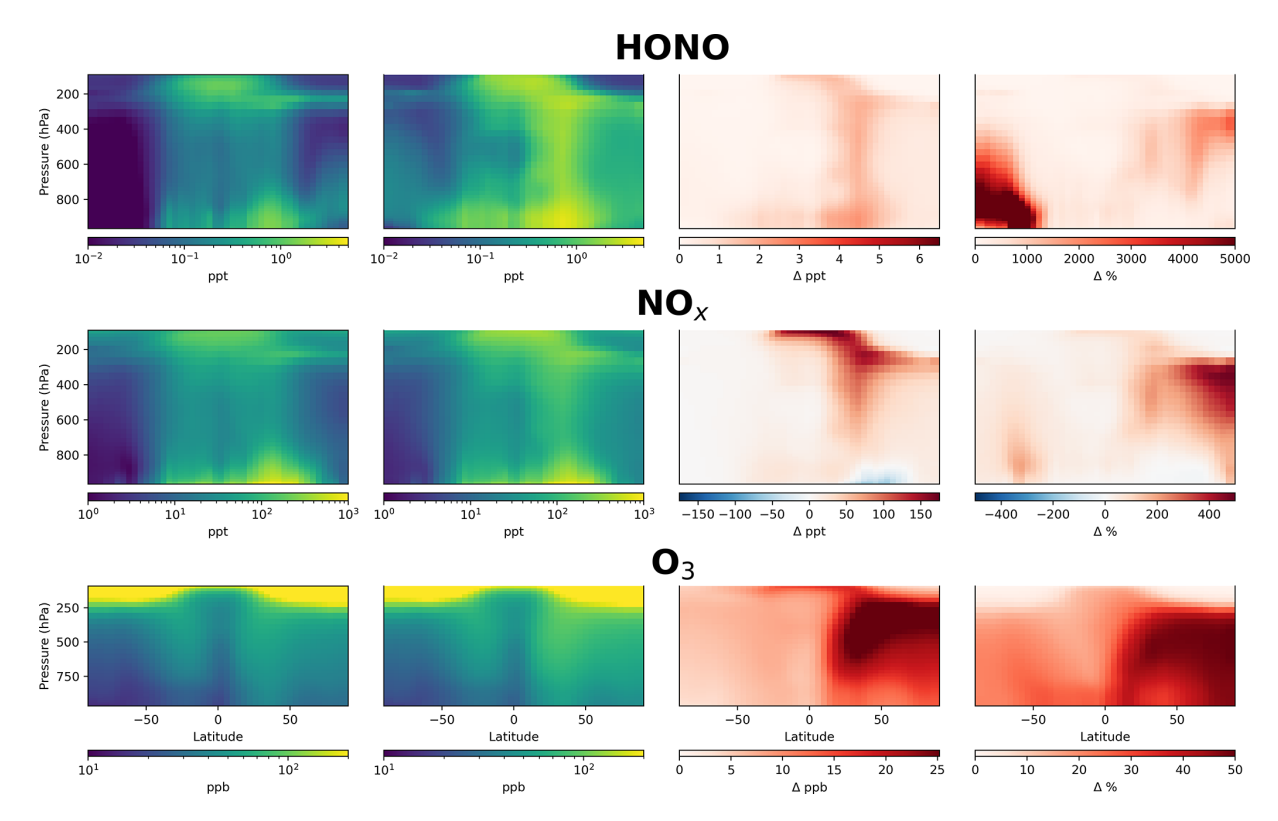


Figure 8. Annual mean zonal concentrations of HONO, NO_x and O_3 in model simulation with (first column) and without (second column) aerosol nitrate photolysis as parameterized by Eq. (1). Absolute difference is shown in the third column and % change in the fourth column.

back into reactive nitrogen (NO_x) . Using our new parameterization, this results in an annual NO_x source almost as large as the total global emission of NO_x (48 TgN yr⁻¹ compared with 55 TgN yr⁻¹) and larger than the anthropogenic (31 TgN yr⁻¹) (Table S1). Unsurprisingly, this large renoxification term has profound implications for atmospheric chemistry, increasing NO_x concentrations globally, as well as tropospheric O_3 production and OH concentrations. The simulated concentrations (Figs. 6, S3). However, our parameterization still underestimates HONO primarily due to the model underestimate of nitrate aerosol concentrations, as discussed above.

The conclusions made here for the chemistry of the atmosphere are significant, thus it is judicious to explore alternative explanations for these findings. Our analyses are dependent on accurate measurements of HONO concentrations in the remote atmosphere. We utilized data from three different techniques and from four independent research groups (see Methods Section) from remote regions where HONO concentrations were above the limit of detection (\sim 1 ppt) to provide robust observations. We note however that HONO observations are often below the limit of detection of current instrumentation; improved technologies would help to provide greater confidence in the lowest concentrations reported. The renoxification mechanism used to simulate the field ob-

servations of HONO shown here is supported by various laboratory estimates of the rate of nitrate photolysis, many of which derive EFs far exceeding those implemented here (Ye et al., 2016, 2017). We note however that even if the nitrate photolysis as applied through this parameterization was overestimated, the observations show that the HONO is significantly higher than the model can reproduce with traditional chemistry. Observations and theory could potentially be reconciled without renoxification if the HONO lifetime (predominantly determined by photolysis) is significantly longer than currently thought. An order of magnitude decrease in the photolysis rate of HONO could essentially remove the disagreement. However, the current photolysis parameters for HONO photolysis (Atkinson et al., 2004) are based on 6 previous studies (Stockwell and Calvert, 1978; Vasudev, 1990; Bongartz et al., 1991; Bongartz et al., 1994; Pagsberg et al., 1997; Wang and Zhang, 2000; Stutz et al., 2000) which agree to within ~ 15 %. Therefore, it is unlikely that the lifetime of HONO is an order of magnitude lower than currently considered, leaving it necessary for other parts of the chemical system to change to remove the inconsistency between HONO observations and observations of O_3 , NO_x , OH etc.

As discussed in the introduction another alternative explanation for the high HONO concentrations could involve a mechanism to convert a NO_x species (NO, NO_2 , NO_3 etc) into HONO rather than the NO_z conversion explored here.

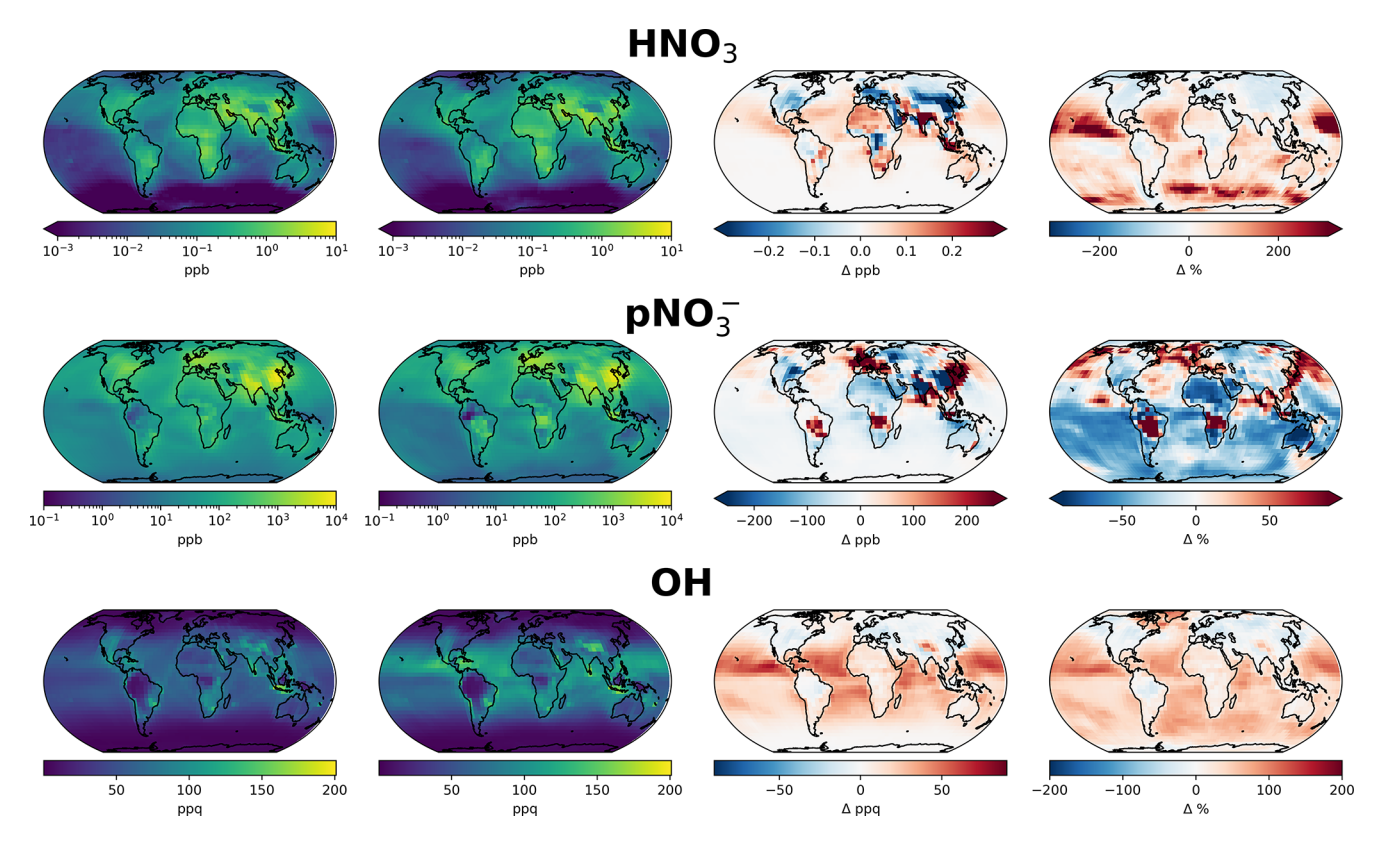


Figure 9. Annual mean surface concentrations of HNO_3 , particulate nitrate (pNO_3^-) and OH in model simulation with (first column) and without (second column) aerosol nitrate photolysis as parameterized by Eq. (1). Absolute difference is shown in the third column and % change in the fourth column.

A number of studies have been discussed in the literature (Crowley and Carl, 1997; Xin et al., 2014; Song et al., 2023) but they remain highly speculative. Most of the impact on the atmospheric composition of nitrate photolysis was felt by the act of converting a relatively long lived NO_z species (NO_3^-) into a short-lived NO_x species (HONO) thus increasing the NO_x concentration. If the HONO was rather produced from the conversion of a NO_x species instead the impact would likely be significantly less. Focused laboratory studies on these potential gas phase conversion routes would be useful to help to rule them in or out of the explanation.

The model's underestimate of total nitrate, but overestimate of fine mode nitrate is another area where model improvements would be useful. The parameterization developed here improves the comparisons with observed fine mode nitrate but does little to change the overall total nitrate underestimate. Improved representation of coarse mode nitrate within the model, which hasn't been a recent priority, will also be needed if the role of nitrate photolysis is to be fully understood.

Increased field observations of HONO in remote environments would also be useful, especially if techniques can be developed which can accurately measure HONO to concentrations significantly lower than currently achieved. Sub ppt concentrations are calculated for the AToM data (Fig. 6) with the new parameterization which is beyond the capabilities of current techniques. HONO concentrations show most sensitivity to the new parameterization in locations such over the remote tropical ocean and the Southern Ocean (See Fig. 7). Making new observations in these location is likely to provide the most utility in helping to constrain this problem.

Assuming that the current nitrate photolysis mechanism is correct, there are potential processes which may decrease NO_x in the atmosphere and thus reconcile this discrepancy. This could either be achieved by decreasing the primary NO_x emission source or by increasing the NO_x sink. Several significant emission sources of NO_x are highly uncertain, including lightning (2–8 Tg yr⁻¹; Murray, 2016; Verma et al., 2021), soil (8.5–15 TgN yr⁻¹; Hudman et al., 2012; Vinken et al., 2014; Weng et al., 2020) and biomass burning (11- $17 \,\mathrm{Tg}\,\mathrm{yr}^{-1}$; Bray et al., 2021). A reduction in these emissions might allow for the NO_x concentrations to be reconciled with the HONO concentrations. From a chemical sink perspective, Butkovskaya et al. (2005) observed in laboratory studies a HNO_3 -forming branch of the $NO + HO_2$ reaction, which reduces NO_x concentrations by ~ 20 %, and resulted in a mean global OH decrease of 13 % and a 5 %-12 % decrease in tropospheric O₃ (Cariolle et al., 2008). Tropospheric halogen chemistry is also uncertain and may contribute to a larger sink for NO_x and O_3 than currently estimated by the model (Iglesias-Suarez et al., 2020; Badia et al., 2021; Wang et al., 2021; Alexander et al., 2020). Stratospheric-tropospheric exchange of O_3 is yet another factor with a large uncertainty, which could account for some of the additional tropospheric O_3 loss required to accommodate the increase due to nitrate photolysis (Wang and Fu, 2021; Ruiz and Prather, 2022). Many of these terms result in small and highly uncertain changes in NO_x , OH and tropospheric O_3 , but together may accommodate the large changes that have resulted from improving modelled HONO relative to measurements and demonstrate a general need for improved understanding of tropospheric chemical processes.

The implication of these results is that our current understanding of the atmospheric chemistry of NO_x , gas phase reactive nitrogen and aerosol phase nitrate is incomplete and needs to be improved if we are to have confidence in our ability to predict the future chemical state of the atmosphere.

Code availability. GEOS-Chem is available from https://github.com/geoschem/geos-chem. The version of the model used is available from: https://doi.org/10.5281/zenodo.12809895 (The International GEOS-Chem User Community, 2024). Updates necessary to run the model are available from https://doi.org/10.5281/zenodo.17483547 (Rowlinson, 2025). Updates necessary to run the model and to produce the plots are available from https://doi.org/10.5281/zenodo.17483547 (Rowlinson, 2025).

Data availability. ARNA data is availble from http://catalogue.ceda.ac.uk/uuid/c3f9945f1c1041f6a20b98940db27335 (last access: 23 November 2025). FIREX data is available from https://doi.org/10.3334/ORNLDAAC/1941 (Hook et al., 2021). ATOM data is available from https://doi.org/10.3334/ORNLDAAC/1581 (Wofsy et al., 2018). Cape Verde data is available from http://catalogue.ceda.ac.uk/uuid/81693aad69409100b1b9a247b9ae75d5 (last access: 23 November 2025).

Supplement. The supplement related to this article is available online at https://doi.org/10.5194/acp-25-16945-2025-supplement.

Author contributions. MJR, LJC, MJE, TS Provided the conceptualization of the study and developed the analysis approach.

JDL, STA, LJC, ABC, RB, WB, SH, LRC, KP, BW, TBR, PRV, PC-J, HG, BAN, JLJ, KWF, provided the observational data used in this study.

MJR, TS, MJE provided model development and methodology. MJR, LJC, MJE Provided the original draft preparation The other authors provided paper review and editing.

Competing interests. At least one of the (co-)authors is a member of the editorial board of *Atmospheric Chemistry and Physics*. The peer-review process was guided by an independent editor, and the authors also have no other competing interests to declare.

Disclaimer. Publisher's note: Copernicus Publications remains neutral with regard to jurisdictional claims made in the text, published maps, institutional affiliations, or any other geographical representation in this paper. While Copernicus Publications makes every effort to include appropriate place names, the final responsibility lies with the authors. Also, please note that this paper has not received English language copy-editing. Views expressed in the text are those of the authors and do not necessarily reflect the views of the publisher.

Acknowledgements. This work was supported by the National Environmental Research Council (NERC) grant NE/S000518/1 to LJC, MJE and JDL. The Cabo Verde Atmospheric Observatory is funded through the National Centre for Atmospheric Science (NCAS). LJC acknowledges funding from the European Research Council (ERC) under the European Union's Horizon 2020 programme (project O3-SML; grant agreement no. 833290). The Viking cluster was used during this project, which is a high-performance compute facility provided by the University of York. We are grateful for computational support from the University of York, IT Services and the Research IT team.

We are grateful for the funding of the HALO aircraft and in particular to the contributions of the German Research Foundation (DFG; HALO-SPP 1294) to the various HALO missions and for the research grants (DFG; grant nos. PF-384/7-1, PF384/9-1, PF-384/16-1, PF-384/17, PF-384/19, PF 384/24-1, and BU 2599/10-1) in support of our measurements from the HALO aircraft.

We acknowledge funding from UK Natural Environment Research Council for the DY151 cruise under the following grants: NE/S00579X/1 (PI Zongbo Shi), NE/S005587/1 (PI Anna Jones), and NE/T00648X/1 (PI Ben Murray). We wish to thank the captain Antione Gatti and the crew of the RRS Discovery, and the National Marine Facility (NMF) team, including NMF technicians (Jon Short, Jack Arnott and Nick Harker) for their support before, during and after the DY151 cruise. We also thank all the science team for their help, discussions and cooperation throughout the campaign.

The CU-Boulder group acknowledges funding from NASA grants 80NSSC21K1451 and 80NSSC23K0828.

The authors would like to thank Glenn Diskin for providing CO measurements used for filtering the FIREX-AQ dataset. We also thank Jack Dibb for providing the FIREX-AQ aerosol filter measurements as well as valuable editorial comments and feedback on the manuscript.

Financial support. This research has been supported by the Natural Environment Research Council (grant nos. NE/S000518/1, NE/S00579X/1, NE/S005587/1, and NE/T00648X/1), the EU HORIZON EUROPE European Research Council (grant no. 833290), the Deutsche Forschungsgemeinschaft (grant nos. PF-384/7-1, PF384/9-1, PF-384/16-1, PF-384/17, PF-384/19, PF

384/24-1, and BU 2599/10-1), and the National Aeronautics and Space Administration (grant nos. 80NSSC21K1451 and 80NSSC23K0828).

Review statement. This paper was edited by Markus Ammann and reviewed by two anonymous referees.

References

- Alexander, B., Sherwen, T., Holmes, C. D., Fisher, J. A., Chen, Q., Evans, M. J., and Kasibhatla, P.: Global inorganic nitrate production mechanisms: comparison of a global model with nitrate isotope observations, Atmos. Chem. Phys., 20, 3859–3877, https://doi.org/10.5194/acp-20-3859-2020, 2020.
- Andersen, S. T., Carpenter, L. J., Nelson, B. S., Neves, L., Read, K. A., Reed, C., Ward, M., Rowlinson, M. J., and Lee, J. D.: Long-term NO_χ measurements in the remote marine tropical troposphere, Atmos. Meas. Tech., 14, 3071–3085, https://doi.org/10.5194/amt-14-3071-2021, 2021.
- Andersen, S. T., Carpenter, L. J., Reed, C., Lee, J. D., Chance,
 R., Sherwen, T., Vaughan, A. R., Stewart, J., Edwards, P. M.,
 Bloss, W. J., Sommariva, R., Crilley, L. R., Nott, G. J., Neves,
 L., Read, K., Heard, D. E., Seakins, P. W., Whalley, L. K.,
 Boustead, G. A., Fleming, L. T., Stone, D., and Fomba, K.
 W.: Extensive field evidence for the release of HONO from the
 photolysis of nitrate aerosols, Science Advances, 9, eadd6266,
 https://doi.org/10.1126/sciadv.add6266, 2023.
- Atkinson, R., Baulch, D. L., Cox, R. A., Crowley, J. N., Hampson, R. F., Hynes, R. G., Jenkin, M. E., Rossi, M. J., and Troe, J.: Evaluated kinetic and photochemical data for atmospheric chemistry: Volume I gas phase reactions of O_x , HO_x , NO_x and SO_x species, Atmos. Chem. Phys., 4, 1461–1738, https://doi.org/10.5194/acp-4-1461-2004, 2004.
- Badia, A., Iglesias-Suarez, F., Fernandez, R. P., Cuevas, C. A., Kinnison, D. E., Lamarque, J.-F., Griffiths, P. T., Tarasick, D. W., Liu, J., and Saiz-Lopez, A.: The Role of Natural Halogens in Global Tropospheric Ozone Chemistry and Budget Under Different 21st Century Climate Scenarios, Journal of Geophysical Research: Atmospheres, 126, e2021JD034859, https://doi.org/10.1029/2021JD034859, 2021.
- Bao, F., Jiang, H., Zhang, Y., Li, M., Ye, C., Wang, W., Ge, M., Chen, C., and Zhao, J.: The Key Role of Sulfate in the Photochemical Renoxification on Real PM_{2.5}, Environmental Science & Technology, 54, 3121–3128, https://doi.org/10.1021/acs.est.9b06764, 2020.
- Bates, K. H., Jacob, D. J., Li, K., Ivatt, P. D., Evans, M. J., Yan, Y., and Lin, J.: Development and evaluation of a new compact mechanism for aromatic oxidation in atmospheric models, Atmos. Chem. Phys., 21, 18351–18374, https://doi.org/10.5194/acp-21-18351-2021, 2021.
- Bekki, S.: On the possible role of aircraft-generated soot in the middle latitude ozone depletion, Journal of Geophysical Research: Atmospheres, 102, 10751–10758, https://doi.org/10.1029/97JD00134, 1997.
- Bey, I., Jacob, D. J., Yantosca, R. M., Logan, J. A., Field, B. D., Fiore, A. M., Li, Q., Liu, H. Y., Mickley, L. J., and Schultz, M. G.: Global modeling of tropospheric chemistry with as-

- similated meteorology: Model description and evaluation, Journal of Geophysical Research: Atmospheres, 106, 23073–23095, https://doi.org/10.1029/2001JD000807, 2001.
- Bongartz, A., Kames, J., Welter, F., and Schurath, U.: Near-UV absorption cross sections and trans/cis equilibrium of nitrous acid, The Journal of Physical Chemistry, 95, 1076–1082, https://doi.org/10.1021/j100156a012, 1991.
- Bongartz, A., Kames, J., Schurath, U., George, C., Mirabel, P., and Ponche, J. L.: Experimental determination of HONO mass accommodation coefficients using two different techniques, Journal of Atmospheric Chemistry, 18, 149–169, https://doi.org/10.1007/BF00696812, 1994.
- Bourgeois, I., Peischl, J., Neuman, J. A., Brown, S. S., Allen, H. M., Campuzano-Jost, P., Coggon, M. M., DiGangi, J. P., Diskin, G. S., Gilman, J. B., Gkatzelis, G. I., Guo, H., Halliday, H. A., Hanisco, T. F., Holmes, C. D., Huey, L. G., Jimenez, J. L., Lamplugh, A. D., Lee, Y. R., Lindaas, J., Moore, R. H., Nault, B. A., Nowak, J. B., Pagonis, D., Rickly, P. S., Robinson, M. A., Rollins, A. W., Selimovic, V., St. Clair, J. M., Tanner, D., Vasquez, K. T., Veres, P. R., Warneke, C., Wennberg, P. O., Washenfelder, R. A., Wiggins, E. B., Womack, C. C., Xu, L., Zarzana, K. J., and Ryerson, T. B.: Comparison of airborne measurements of NO, NO₂, HONO, NO_y, and CO during FIREX-AQ, Atmos. Meas. Tech., 15, 4901–4930, https://doi.org/10.5194/amt-15-4901-2022, 2022.
- Bousquet, P., Hauglustaine, D. A., Peylin, P., Carouge, C., and Ciais, P.: Two decades of OH variability as inferred by an inversion of atmospheric transport and chemistry of methyl chloroform, Atmos. Chem. Phys., 5, 2635–2656, https://doi.org/10.5194/acp-5-2635-2005, 2005.
- Bray, C. D., Battye, W. H., Aneja, V. P., and Schlesinger, W. H.: Global emissions of NH₃, NO_x, and N₂O from biomass burning and the impact of climate change, Journal of the Air & Waste Management Association, 71, 102–114, https://doi.org/10.1080/10962247.2020.1842822, 2021.
- Butkovskaya, N. I., Kukui, A., Pouvesle, N., and Le Bras, G.: Formation of Nitric Acid in the Gas-Phase HO₂ + NO Reaction: Effects of Temperature and Water Vapor, The Journal of Physical Chemistry A, 109, 6509–6520, https://doi.org/10.1021/jp051534v, 2005.
- Cariolle, D., Evans, M. J., Chipperfield, M. P., Butkovskaya, N., Kukui, A., and Le Bras, G.: Impact of the new HNO₃-forming channel of the $HO_2 + NO$ reaction on tropospheric HNO_3 , NO_x , HO_x and ozone, Atmos. Chem. Phys., 8, 4061–4068, https://doi.org/10.5194/acp-8-4061-2008, 2008.
- Carpenter, L. J., Fleming, Z. L., Read, K. A., Lee, J. D., Moller, S. J., Hopkins, J. R., Purvis, R. M., Lewis, A. C., Moller, K., Heinold, B., Herrmann, H., Fomba, K. W., van Pinxteren, D., Müller, C., Tegen, I., Wiedensohler, A., Müller, T., Niedermeier, N., Achterberg, E. P., Patey, M. D., Kozlova, E. A., Heimann, M., Heard, D. E., Plane, J. M. C., Mahajan, A., Oetjen, H., Ingham, T., Stone, D., Whalley, L. K., Evans, M. J., Pilling, M. J., Leigh, R. J., Monks, P. S., Karunaharan, A., Vaughan, S., Arnold, S. R., Tschritter, J., Pöhler, D., Frieß, U., Holla, R., Mendes, L. M., Lopez, H., Faria, B., Manning, A. J., and Wallace, D. W. R.: Seasonal characteristics of tropical marine boundary layer air measured at the Cape Verde Atmospheric Observatory, Journal of Atmospheric Chemistry, 67, 87–140, https://doi.org/10.1007/s10874-011-9206-1, 2010.

- Cressot, C., Chevallier, F., Bousquet, P., Crevoisier, C., Dlugo-kencky, E. J., Fortems-Cheiney, A., Frankenberg, C., Parker, R., Pison, I., Scheepmaker, R. A., Montzka, S. A., Krummel, P. B., Steele, L. P., and Langenfelds, R. L.: On the consistency between global and regional methane emissions inferred from SCIAMACHY, TANSO-FTS, IASI and surface measurements, Atmos. Chem. Phys., 14, 577–592, https://doi.org/10.5194/acp-14-577-2014, 2014.
- Crilley, L. R., Kramer, L. J., Pope, F. D., Reed, C., Lee, J. D., Carpenter, L. J., Hollis, L. D. J., Ball, S. M., and Bloss, W. J.: Is the ocean surface a source of nitrous acid (HONO) in the marine boundary layer?, Atmos. Chem. Phys., 21, 18213–18225, https://doi.org/10.5194/acp-21-18213-2021, 2021.
- Crowley, J. N. and Carl, S. A.: OH formation in the photoexcitation of NO₂ beyond the dissociation threshold in the presence of water vapor, J. Phys. Chem., 101, 4178–4184, 1997.
- Dang, R., Jacob, D. J., Shah, V., Eastham, S. D., Fritz, T. M., Mickley, L. J., Liu, T., Wang, Y., and Wang, J.: Background nitrogen dioxide (NO₂) over the United States and its implications for satellite observations and trends: effects of nitrate photolysis, aircraft, and open fires, Atmos. Chem. Phys., 23, 6271–6284, https://doi.org/10.5194/acp-23-6271-2023, 2023.
- Dibb, J. E., Jaffrezo, J. L., and Bergin, M. H.: ATM aerosol concentrations around the GISP ice core site, PANGEA [data set], https://doi.org/10.1594/PANGAEA.56077, 1999.
- Dibb, J. E., Talbot, R. W., Seid, G., Jordan, C., Scheuer, E., Atlas, E., Blake, N. J., and Blake, D. R.: Airborne sampling of aerosol particles: Comparison between surface sampling at Christmas Island and P-3 sampling during PEM-Tropics B, Journal of Geophysical Research: Atmospheres, 107, PEM 2–1–PEM 2–17, https://doi.org/10.1029/2001JD000408, 2002.
- Dillon, T. J. and Crowley, J. N.: Reactive quenching of electronically excited NO_2^* and NO_3^* by H_2O as potential sources of atmospheric HOx radicals, Atmos. Chem. Phys., 18, 14005–14015, https://doi.org/10.5194/acp-18-14005-2018, 2018.
- Du, J. and Zhu, L.: Quantification of the absorption cross sections of surface-adsorbed nitric acid in the 335–365 nm region by Brewster angle cavity ring-down spectroscopy, Chemical Physics Letters, 511, 213–218, https://doi.org/10.1016/j.cplett.2011.06.062, 2011.
- Fomba, K. W., Müller, K., van Pinxteren, D., Poulain, L., van Pinxteren, M., and Herrmann, H.: Long-term chemical characterization of tropical and marine aerosols at the Cape Verde Atmospheric Observatory (CVAO) from 2007 to 2011, Atmos. Chem. Phys., 14, 8883–8904, https://doi.org/10.5194/acp-14-8883-2014, 2014.
- Gao, C. Y., Heald, C. L., Katich, J. M., Luo, G., and Yu, F.: Remote Aerosol Simulated During the Atmospheric Tomography (ATom) Campaign and Implications for Aerosol Lifetime, Journal of Geophysical Research: Atmospheres, 127, e2022JD036524, https://doi.org/10.1029/2022JD036524, 2022.
- Gelaro, R., McCarty, W., Suárez, M. J., Todling, R., Molod, A., Takacs, L., Randles, C. A., Darmenov, A., Bosilovich, M. G., Reichle, R., Wargan, K., Coy, L., Cullather, R., Draper, C., Akella, S., Buchard, V., Conaty, A., da Silva, A. M., Gu, W., Kim, G.-K., Koster, R., Lucchesi, R., Merkova, D., Nielsen, J. E., Partyka, G., Pawson, S., Putman, W., Rienecker, M., Schubert, S. D., Sienkiewicz, M., and Zhao, B.: The Modern-Era Retrospective Analysis for Research and Applications,

- Version 2 (MERRA-2), Journal of Climate, 30, 5419–5454, https://doi.org/10.1175/JCLI-D-16-0758.1, 2017.
- Gen, M., Liang, Z., Zhang, R., Go, B. R., and Chan, C. K.: Particulate nitrate photolysis in the atmosphere, Environ. Sci.: Atmos., 2, 111–127, https://doi.org/10.1039/D1EA00087J, 2022.
- Guenther, A., Hewitt, C. N., Erickson, D., Fall, R., Geron, C., Graedel, T., Harley, P., Klinger, L., Lerdau, M., Mckay, W. A., Pierce, T., Scholes, B., Steinbrecher, R., Tallamraju, R., Taylor, J., and Zimmerman, P.: A global model of natural volatile organic compound emissions, Journal of Geophysical Research: Atmospheres, 100, 8873–8892, https://doi.org/10.1029/94JD02950, 1995.
- Guo, H., Campuzano-Jost, P., Nault, B. A., Day, D. A., Schroder, J. C., Kim, D., Dibb, J. E., Dollner, M., Weinzierl, B., and Jimenez, J. L.: The importance of size ranges in aerosol instrument intercomparisons: a case study for the Atmospheric Tomography Mission, Atmos. Meas. Tech., 14, 3631–3655, https://doi.org/10.5194/amt-14-3631-2021, 2021.
- Heland, J., Kleffmann, J., Kurtenbach, R., and Wiesen, P.: A New Instrument To Measure Gaseous Nitrous Acid (HONO) in the Atmosphere, Environmental Science & Technology, 35, 3207– 3212, https://doi.org/10.1021/es000303t, 2001.
- Hoesly, R. M., Smith, S. J., Feng, L., Klimont, Z., Janssens-Maenhout, G., Pitkanen, T., Seibert, J. J., Vu, L., Andres, R. J., Bolt, R. M., Bond, T. C., Dawidowski, L., Kholod, N., Kurokawa, J.-I., Li, M., Liu, L., Lu, Z., Moura, M. C. P., O'Rourke, P. R., and Zhang, Q.: Historical (1750–2014) anthropogenic emissions of reactive gases and aerosols from the Community Emissions Data System (CEDS), Geosci. Model Dev., 11, 369–408, https://doi.org/10.5194/gmd-11-369-2018, 2018.
- Hook, S. J., Myers, J. S., Thome, K. J., Fitzgerald, M., Kahle, A. B., Airborne Sensor Facility NASA Ames Research Center, Crawford, J. H., Warneke, C., and Schwarz, J. P.: MASTER: FIREX-AQ Airborne Campaign, Western-Central USA, Summer 2019 (Version 1.2), ORNL Distributed Active Archive Center [data set], https://doi.org/10.3334/ORNLDAAC/1941, 2021.
- Hua, W., Verreault, D., and Allen, H. C.: Surface Electric Fields of Aqueous Solutions of NH₄NO₃, Mg(NO₃)₂, NaNO₃, and LiNO₃: Implications for Atmospheric Aerosol Chemistry, The Journal of Physical Chemistry C, 118, 24941–24949, https://doi.org/10.1021/jp505770t, 2014.
- Hudman, R. C., Moore, N. E., Mebust, A. K., Martin, R. V., Russell, A. R., Valin, L. C., and Cohen, R. C.: Steps towards a mechanistic model of global soil nitric oxide emissions: implementation and space based-constraints, Atmos. Chem. Phys., 12, 7779–7795, https://doi.org/10.5194/acp-12-7779-2012, 2012.
- Iglesias-Suarez, F., Badia, A., Fernandez, R. P., Cuevas, C. A., Kinnison, D. E., Tilmes, S., Lamarque, J.-F., Long, M. C., Hossaini, R., and Saiz-Lopez, A.: Natural halogens buffer tropospheric ozone in a changing climate, Nature Climate Change, 10, 147–154, https://doi.org/10.1038/s41558-019-0675-6, 2020.
- Ivatt, P. D., Evans, M. J., and Lewis, A. C.: Suppression of surface ozone by an aerosol-inhibited photochemical ozone regime, Nature Geoscience, 15, 536–540, https://doi.org/10.1038/s41561-022-00972-9, 2022.
- Jiang, Y., Hoffmann, E. H., Tilgner, A., Aiyuk, M. B. E., Andersen, S. T., Wen, L., van Pinxteren, M., Shen, H., Xue, L., Wang, W., and Herrmann, H.: Insights Into NO_x and HONO Chemistry in the Tropical Marine Boundary Layer

- at Cape Verde During the MarParCloud Campaign, Journal of Geophysical Research-Atmospheres, 128, e2023JD038865, https://doi.org/10.1029/2023JD038865, 2023.
- Jiang, Y., Xia, M., Xue, L., Wang, X., Zhong, X., Liu, Y., Kulmala, M., Ma, T., Wang, J., Wang, Y., Gao, J., and Wang, T.: Quantifying HONO Production from Nitrate Photolysis in a Polluted Atmosphere, Environmental Science & Technology, 58, 14361–14371, https://doi.org/10.1021/acs.est.4c06061, 2024.
- Kasibhatla, P., Sherwen, T., Evans, M. J., Carpenter, L. J., Reed, C., Alexander, B., Chen, Q., Sulprizio, M. P., Lee, J. D., Read, K. A., Bloss, W., Crilley, L. R., Keene, W. C., Pszenny, A. A. P., and Hodzic, A.: Global impact of nitrate photolysis in sea-salt aerosol on NO_x, OH, and O₃ in the marine boundary layer, Atmos. Chem. Phys., 18, 11185–11203, https://doi.org/10.5194/acp-18-11185-2018, 2018.
- Kleffmann, J.: Daytime Sources of Nitrous Acid (HONO) in the Atmospheric Boundary Layer, Chem. Phys. Chem., 8, 1137–1144, https://doi.org/10.1002/cphc.200700016, 2007.
- Kleffmann, J. and Wiesen, P.: Technical Note: Quantification of interferences of wet chemical HONO LOPAP measurements under simulated polar conditions, Atmos. Chem. Phys., 8, 6813–6822, https://doi.org/10.5194/acp-8-6813-2008, 2008.
- Knipping, E. M. and Dabdub, D.: Modeling surface-mediated renoxification of the atmosphere via reaction of gaseous nitric oxide with deposited nitric acid, Atmospheric Environment, 36, 5741–5748, https://doi.org/10.1016/S1352-2310(02)00652-0, 2002.
- Lary, D. J., Lee, A. M., Toumi, R., Newchurch, M. J., Pirre, M., and Renard, J. B.: Carbon aerosols and atmospheric photochemistry, Journal of Geophysical Research: Atmospheres, 102, 3671–3682, https://doi.org/10.1029/96JD02969, 1997.
- Lee, B. H., Lopez-Hilfiker, F. D., Mohr, C., Kurtén, T., Worsnop, D. R., and Thornton, J. A.: An Iodide-Adduct High-Resolution Time-ofFlight Chemical-Ionization Mass Spectrometer: Application to Atmospheric Inorganic and Organic Compounds, Environmental Science & Technology, 48, 6309–6317, https://doi.org/10.1021/es500362a, 2014.
- Li, B., Gao, J., Chen, C., Wen, L., Zhang, Y., Li, J., Zhang, Y., Du, X., Zhang, K., and Wang, J.: Exploring HONO production from particulate nitrate photolysis in representative regions of China: characteristics, influencing factors, and environmental implications, Atmos. Chem. Phys., 24, 13183–13198, https://doi.org/10.5194/acp-24-13183-2024, 2024.
- Liu, J., Li, S., Mekic, M., Jiang, H., Zhou, W., Loisel, G., Song, W., Wang, X., and Gligorovski, S.: Photo enhanced uptake of NO₂ and HONO formation on real urban grime, Environmental Science & Technology Letters, 6, 413–417, 2019,
- McDuffie, E. E., Smith, S. J., O'Rourke, P., Tibrewal, K., Venkataraman, C., Marais, E. A., Zheng, B., Crippa, M., Brauer, M., and Martin, R. V.: A global anthropogenic emission inventory of atmospheric pollutants from sector- and fuel-specific sources (1970–2017): an application of the Community Emissions Data System (CEDS), Earth Syst. Sci. Data, 12, 3413–3442, https://doi.org/10.5194/essd-12-3413-2020, 2020.
- Meinshausen, M., Vogel, E., Nauels, A., Lorbacher, K., Meinshausen, N., Etheridge, D. M., Fraser, P. J., Montzka, S. A., Rayner, P. J., Trudinger, C. M., Krummel, P. B., Beyerle, U., Canadell, J. G., Daniel, J. S., Enting, I. G., Law, R. M., Lunder, C. R., O'Doherty, S., Prinn, R. G., Reimann, S., Rubino,

- M., Velders, G. J. M., Vollmer, M. K., Wang, R. H. J., and Weiss, R.: Historical greenhouse gas concentrations for climate modelling (CMIP6), Geosci. Model Dev., 10, 2057–2116, https://doi.org/10.5194/gmd-10-2057-2017, 2017.
- Meng, Z., Dabdub, D., and Seinfeld, J. H.: Chemical Coupling Between Atmospheric Ozone and Particulate Matter, Science, 277, 116–119, https://doi.org/10.1126/science.277.5322.116, 1997.
- Miao, R., Chen, Q., Zheng, Y., Cheng, X., Sun, Y., Palmer, P. I., Shrivastava, M., Guo, J., Zhang, Q., Liu, Y., Tan, Z., Ma, X., Chen, S., Zeng, L., Lu, K., and Zhang, Y.: Model bias in simulating major chemical components of PM_{2.5} in China, Atmos. Chem. Phys., 20, 12265–12284, https://doi.org/10.5194/acp-20-12265-2020, 2020.
- Monks, P. S., Archibald, A. T., Colette, A., Cooper, O., Coyle, M., Derwent, R., Fowler, D., Granier, C., Law, K. S., Mills, G. E., Stevenson, D. S., Tarasova, O., Thouret, V., von Schneidemesser, E., Sommariva, R., Wild, O., and Williams, M. L.: Tropospheric ozone and its precursors from the urban to the global scale from air quality to short-lived climate forcer, Atmos. Chem. Phys., 15, 8889–8973, https://doi.org/10.5194/acp-15-8889-2015, 2015.
- Murray, L. T.: Lightning NO_x and Impacts on Air Quality, Current Pollution Reports, 2, 115–133, https://doi.org/10.1007/s40726-016-0031-7, 2016.
- Murray, L. T., Logan, J. A., and Jacob, D. J.: Interannual variability in tropical tropospheric ozone and OH: The role of lightning, Journal of Geophysical Research: Atmospheres, 118, 11468–11480, https://doi.org/10.1002/jgrd.50857, 2013.
- Myhre, G., Shindell, D., Bréon, F.-M., Collins, W., Fuglestvedt, J., Huang, J., Koch, D., Lamarque, J.-F., Lee, D., Mendoza, B., Nakajima, T., Robock, A., Stephens, G., Takemura, T., and Zhang, H.: Anthropogenic and natural radiative forcing, Cambridge University Press, Cambridge, UK, 659–740, https://doi.org/10.1017/CBO9781107415324.018, 2013.
- Naik, V., Voulgarakis, A., Fiore, A. M., Horowitz, L. W., Lamarque, J.-F., Lin, M., Prather, M. J., Young, P. J., Bergmann, D., Cameron-Smith, P. J., Cionni, I., Collins, W. J., Dalsøren, S. B., Doherty, R., Eyring, V., Faluvegi, G., Folberth, G. A., Josse, B., Lee, Y. H., MacKenzie, I. A., Nagashima, T., van Noije, T. P. C., Plummer, D. A., Righi, M., Rumbold, S. T., Skeie, R., Shindell, D. T., Stevenson, D. S., Strode, S., Sudo, K., Szopa, S., and Zeng, G.: Preindustrial to present-day changes in tropospheric hydroxyl radical and methane lifetime from the Atmospheric Chemistry and Climate Model Intercomparison Project (ACCMIP), Atmos. Chem. Phys., 13, 5277–5298, https://doi.org/10.5194/acp-13-5277-2013, 2013.
- Nault, B. A., Campuzano-Jost, P., Day, Douglas A.and Jo, D. S., Schroder, J. C., Allen, H. M., Bahreini, R., Bian, H., Blake, D. R., Chin, M., Clegg, S. L., Colarco, P. R., Crounse, J. D., Cubison, M. J., DeCarlo, P. F., Dibb, J. E., Diskin, G. S., Hodzic, A., Hu, W., Katich, J. M., Kim, M. J., Kodros, J. K., Kupc, A., Lopez-Hilfiker, F. D., Marais, E. A., Middlebrook, A. M., Andrew Neuman, J., Nowak, J. B., Palm, B. B., Paulot, F., Pierce, J. R., Schill, Gregory P. and Scheuer, E., Thornton, J. A., Tsigaridis, K., Wennberg, P. O., Williamson, C. J., and Jimenez, J. L.: Chemical transport models often underestimate inorganic aerosol acidity in remote regions of the atmosphere, Communications Earth & Environment, 2, 93, https://doi.org/10.1038/s43247-021-00164-0, 2021.

- Ndour, M., Conchon, P., D'Anna, B., Ka, O., and George, C.: Photochemistry of mineral dust surface as a potential atmospheric renoxification process, Geophysical Research Letters, 36, https://doi.org/10.1029/2008GL036662, 2009.
- Nguyen, D.-H., Lin, C., Vu, C.-T., Cheruiyot, N. K., Nguyen, M. K., Le, T. H., Lukkhasorn, W., Vo, T.-D.-H., and Bui, X.-T.: Tropospheric ozone and NOx: A review of worldwide variation and meteorological influences, Environmental Technology and Innovation, 28, 102809, https://doi.org/10.1016/j.eti.2022.102809, 2022.
- Ninneman, M., Lu, S., Zhou, X., and Schwab, J.: On the Importance of Surface-Enhanced Renoxification as an Oxides of Nitrogen Source in Rural and Urban New York State, ACS Earth and Space Chemistry, 4, 1985–1992, https://doi.org/10.1021/acsearthspacechem.0c00185, 2020.
- Pagsberg, P., Bjergbakke, E., Ratajczak, E., and Sillesen, A.: Kinetics of the gas phase reaction OH + NO(+M) → HONO(+M) and the determination of the UV absorption cross sections of HONO, Chemical Physics Letters, 272, 383–390, https://doi.org/10.1016/S0009-2614(97)00576-9, 1997.
- Parrish, D. D., Norton, R. B., Bollinger, M. J., Liu, S. C., Murphy, P. C., Albritton, D. L., Fehsenfeld, F. C., and Huebert, B. J.: Measurements of HNO₃ and NO₃ particulates at a rural site in the Colorado mountains, Journal of Geophysical Research: Atmospheres, 91, 5379–5393, https://doi.org/10.1029/JD091iD05p05379, 1986.
- Patra, P. K., Krol, M. C., Montzka, S. A., Arnold, T., Atlas, E. L., Lintner, B. R., Stephens, B. B., Xiang, B., Elkins, J. W., Fraser, P. J., Ghosh, A., Hintsa, E. J., Hurst, D. F., Ishijima, K., Krummel, P. B., Miller, B. R., Miyazaki, K., Moore, F. L., Mühle, J., O,ÄôDoherty, S., Prinn, R. G., Steele, L. P., Takigawa, M., Wang, H. J., Weiss, R. F., Wofsy, S. C., and Young, D.: Observational evidence for interhemispheric hydroxyl-radical parity, Nature, 513, 219–223, https://doi.org/10.1038/nature13721, 2014.
- Prospero, J. M.: Long-range transport of mineral dust in the global atmosphere: Impact of African dust on the environment of the southeastern United States, Proc. Natl. Acad. Sci. USA, 96, 3396–3403, https://doi.org/10.1073/pnas.96.7.3396, 1999.
- Prospero, J. M. and Lamb, P. J.: African Droughts and Dust Transport to the Caribbean: Climate Change Implications, Science, 302, 1024–1027, https://doi.org/10.1126/science.1089915, 2003.
- Ramazan, K. A., Wingen, L. M., Miller, Y., Chaban, G. M., Gerber, R. B., Xantheas, S. S., and Finlayson-Pitts, B. J.: New Experimental and Theoretical Approach to the Heterogeneous Hydrolysis of NO₂: Key Role of Molecular Nitric Acid and Its Complexes, The Journal of Physical Chemistry A, 110, 6886–6897, https://doi.org/10.1021/jp056426n, 2006.
- Reed, C., Brumby, C. A., Crilley, L. R., Kramer, L. J., Bloss, W. J., Seakins, P. W., Lee, J. D., and Carpenter, L. J.: HONO measurement by differential photolysis, Atmos. Meas. Tech., 9, 2483– 2495, https://doi.org/10.5194/amt-9-2483-2016, 2016.
- Reed, C., Evans, M. J., Crilley, L. R., Bloss, W. J., Sherwen, T., Read, K. A., Lee, J. D., and Carpenter, L. J.: Evidence for renoxification in the tropical marine boundary layer, Atmos. Chem. Phys., 17, 4081–4092, https://doi.org/10.5194/acp-17-4081-2017, 2017.
- Richards, N. K. and Finlayson-Pitts, B. J.: Production of Gas Phase NO₂ and Halogens from the Photochemical Oxidation of Aqueous Mixtures of Sea Salt and Nitrate Ions at Room Tempera-

- ture, Environmental Science & Technology, 46, 10447–10454, https://doi.org/10.1021/es300607c, 2012.
- Richards, N. K., Wingen, L. M., Callahan, K. M., Nishino, N., Kleinman, M. T., Tobias, D. J., and Finlayson-Pitts, B. J.: Nitrate ion photolysis in thin water films in the presence of bromide ions, J. Phys. Chem. A, 115, 5810–5821, 2011.
- Rowlinson, M.: Code used for "A nitrate photolysis source of tropospheric HONO is incompatible with current understanding of atmospheric chemistry" Rowlinson et al., Zenodo [code and data set], https://doi.org/10.5281/zenodo.17483547, 2025.
- Ruiz, D. J. and Prather, M. J.: From the middle stratosphere to the surface, using nitrous oxide to constrain the stratosphere–troposphere exchange of ozone, Atmos. Chem. Phys., 22, 2079–2093, https://doi.org/10.5194/acp-22-2079-2022, 2022.
- Sachse, G. W., Hill, G. F., Wade, L. O., and Perry, M. G.: Fast-response, high-precision carbon monoxide sensor using a tunable diode laser absorption technique, Journal of Geophysical Research: Atmospheres, 92, 2071–2081, https://doi.org/10.1029/JD092iD02p02071, 1987.
- Sachse Jr., G. W., J. E. C., Hill, G. F., Wade, L. O., Burney, L. G., and Ritter, J. A.: Airborne tunable diode laser sensor for high-precision concentration and flux measurements of carbon monoxide and methane, in: Measurement of Atmospheric Gases, edited by: Schiff, H. I., vol. 1433, International Society for Optics and Photonics, SPIE, 157–166, https://doi.org/10.1117/12.46162, 1991.
- Saunois, M., Stavert, A. R., Poulter, B., Bousquet, P., Canadell, J. G., Jackson, R. B., Raymond, P. A., Dlugokencky, E. J., Houweling, S., Patra, P. K., Ciais, P., Arora, V. K., Bastviken, D., Bergamaschi, P., Blake, D. R., Brailsford, G., Bruhwiler, L., Carlson, K. M., Carrol, M., Castaldi, S., Chandra, N., Crevoisier, C., Crill, P. M., Covey, K., Curry, C. L., Etiope, G., Frankenberg, C., Gedney, N., Hegglin, M. I., Höglund-Isaksson, L., Hugelius, G., Ishizawa, M., Ito, A., Janssens-Maenhout, G., Jensen, K. M., Joos, F., Kleinen, T., Krummel, P. B., Langenfelds, R. L., Laruelle, G. G., Liu, L., Machida, T., Maksyutov, S., McDonald, K. C., McNorton, J., Miller, P. A., Melton, J. R., Morino, I., Müller, J., Murguia-Flores, F., Naik, V., Niwa, Y., Noce, S., O'Doherty, S., Parker, R. J., Peng, C., Peng, S., Peters, G. P., Prigent, C., Prinn, R., Ramonet, M., Regnier, P., Riley, W. J., Rosentreter, J. A., Segers, A., Simpson, I. J., Shi, H., Smith, S. J., Steele, L. P., Thornton, B. F., Tian, H., Tohjima, Y., Tubiello, F. N., Tsuruta, A., Viovy, N., Voulgarakis, A., Weber, T. S., van Weele, M., van der Werf, G. R., Weiss, R. F., Worthy, D., Wunch, D., Yin, Y., Yoshida, Y., Zhang, W., Zhang, Z., Zhao, Y., Zheng, B., Zhu, Q., Zhu, Q., and Zhuang, Q.: The Global Methane Budget 2000-2017, Earth Syst. Sci. Data, 12, 1561-1623, https://doi.org/10.5194/essd-12-1561-2020, 2020.
- Savoie, D. L., Arimoto, R., Keene, W. C., Prospero, J. M., Duce, R. A., and Galloway, J. N.: Marine biogenic and anthropogenic contributions to non-sea-salt sulfate in the marine boundary layer over the North Atlantic Ocean, J. Geophys. Res., 107, 4356, https://doi.org/10.1029/2001JD000970, 2002.
- Scheuer, E., Talbot, R. W., Dibb, J. E., Seid, G. K., De-Bell, L., and Lefer, B.: Seasonal distributions of fine aerosol sulfate in the North American Arctic basin during TOPSE, Journal of Geophysical Research: Atmospheres, 108, https://doi.org/10.1029/2001JD001364, 2003.

- Shah, V., Jacob, D. J., Dang, R., Lamsal, L. N., Strode, S. A., Steenrod, S. D., Boersma, K. F., Eastham, S. D., Fritz, T. M., Thompson, C., Peischl, J., Bourgeois, I., Pollack, I. B., Nault, B. A., Cohen, R. C., Campuzano-Jost, P., Jimenez, J. L., Andersen, S. T., Carpenter, L. J., Sherwen, T., and Evans, M. J.: Nitrogen oxides in the free troposphere: implications for tropospheric oxidants and the interpretation of satellite NO₂ measurements, Atmos. Chem. Phys., 23, 1227–1257, https://doi.org/10.5194/acp-23-1227-2023, 2023.
- Shah, V., Keller, C. A., Knowland, K. E., Christiansen, A., Hu, L., Wang, H., Lu, X., Alexander, B., and Jacob, D. J.: Particulate Nitrate Photolysis as a Possible Driver of Rising Tropospheric Ozone, Geophysical Research Letters, 51, e2023GL107980, https://doi.org/10.1029/2023GL107980, 2024.
- Shi, Q., Tao, Y., Krechmer, J. E., Heald, C. L., Murphy, J. G., Kroll, J. H., and Ye, Q.: Laboratory Investigation of Renoxification from the Photolysis of Inorganic Particulate Nitrate, Environmental Science & Technology, 55, 854–861, https://doi.org/10.1021/acs.est.0c06049, 2021.
- Sillman, S. and He, D.: Some theoretical results concerning O₃-NO-VOC chemistry and NO-VOC indicators, Journal of Geophysical Research: Atmospheres, 107, ACH 26-1–ACH 26-15, https://doi.org/10.1029/2001JD001123, 2002.
- Sommariva, R., Alam, M. S., Crilley, L. R., Rooney, D. J., Bloss, W. J., Fomba, K. W., Andersen, S. T., and Carpenter, L. J.: Factors Influencing the Formation of Nitrous Acid from Photolysis of Particulate Nitrate, The Journal of Physical Chemistry A, 127, 9302–9310, https://doi.org/10.1021/acs.jpca.3c03853, 2023.
- Song, M., Zhao, X., Liu, P., Mu, J., He, G., Zhang, C., Tong, S., Xue, C., Zhao, X., Ge, M., and Mu, Y.: Atmospheric NO_χ oxidation as major sources for nitrous acid (HONO), Npj Climate and Atmospheric Science, 6, 30, https://doi.org/10.1038/s41612-023-00357-8, 2023.
- Stavrakou, T., Müller, J.-F., Boersma, K. F., van der A, R. J., Kurokawa, J., Ohara, T., and Zhang, Q.: Key chemical NO_X sink uncertainties and how they influence top-down emissions of nitrogen oxides, Atmos. Chem. Phys., 13, 9057–9082, https://doi.org/10.5194/acp-13-9057-2013, 2013.
- Stevenson, D. S., Young, P. J., Naik, V., Lamarque, J.-F., Shindell, D. T., Voulgarakis, A., Skeie, R. B., Dalsoren, S. B., Myhre, G., Berntsen, T. K., Folberth, G. A., Rumbold, S. T., Collins, W. J., MacKenzie, I. A., Doherty, R. M., Zeng, G., van Noije, T. P. C., Strunk, A., Bergmann, D., Cameron-Smith, P., Plummer, D. A., Strode, S. A., Horowitz, L., Lee, Y. H., Szopa, S., Sudo, K., Nagashima, T., Josse, B., Cionni, I., Righi, M., Eyring, V., Conley, A., Bowman, K. W., Wild, O., and Archibald, A.: Tropospheric ozone changes, radiative forcing and attribution to emissions in the Atmospheric Chemistry and Climate Model Intercomparison Project (ACCMIP), Atmos. Chem. Phys., 13, 3063–3085, https://doi.org/10.5194/acp-13-3063-2013, 2013.
- Stockwell, W. R. and Calvert, J. G.: The near ultraviolet absorption spectrum of gaseous HONO and N_2O_3 , Journal of Photochemistry, 8, 193–203, https://doi.org/10.1016/0047-2670(78)80019-7, 1978.
- Stutz, J., Kim, E. S., Platt, U., Bruno, P., Perrino, C., and Febo, A.: UV-visible absorption cross sections of nitrous acid, Journal of Geophysical Research: Atmospheres, 105, 14585–14592, https://doi.org/10.1029/2000JD900003, 2000.

- Szopa, S., Naik, V., Adhikary, B., Artaxo, P., Berntsen, T., Collins, W., Fuzzi, S., Gallardo, L., Kiendler-Scharr, A., Klimont, Z., Liao, H., Unger, N., and Zanis, P.: Short-Lived Climate Forcers, in: Climate Change 2021: The Physical Science Basis. Contribution of Working Group I to the Sixth Assessment Report of the Intergovernmental Panel on Climate Change, Report, IPCC, https://doi.org/10.1017/9781009157896.008, 2021.
- The International GEOS-Chem User Community: geoschem/GCClassic: GCClassic 14.4.2, Zenodo [code], https://doi.org/10.5281/zenodo.12809895, 2024.
- Thompson, C. R., Wofsy, S. C., Prather, M. J., Newman, P. A., Hanisco, T. F., Ryerson, T. B., Fahey, D. W., Apel, E. C., Brock, C. A., Brune, W. H., Froyd, K., Katich, J. M., Nicely, J. M., Peischl, J., Ray, E., Veres, P. R., Wang, S., Allen, H. M., Asher, E., Bian, H., Blake, D., Bourgeois, I., Budney, J., Bui, T. P., Butler, A., Campuzano-Jost, P., Chang, C., Chin, M., Commane, R., Correa, G., Crounse, J. D., Daube, B., Dibb, J. E., DiGangi, J. P., Diskin, G. S., Dollner, M., Elkins, J. W., Fiore, A. M., Flynn, C. M., Guo, H., Hall, S. R., Hannun, R. A., Hills, A., Hintsa, E. J., Hodzic, A., Hornbrook, R. S., Huey, L. G., Jimenez, J. L., Keeling, R. F., Kim, M. J., Kupc, A., Lacey, F., Lait, L. R., Lamarque, J.-F., Liu, J., McKain, K., Meinardi, S., Miller, D. O., Montzka, S. A., Moore, F. L., Morgan, E. J., Murphy, D. M., Murray, L. T., Nault, B. A., Neuman, J. A., Nguyen, L., Gonzalez, Y., Rollins, A., Rosenlof, K., Sargent, M., Schill, G., Schwarz, J. P., Clair, J. M. S., Steenrod, S. D., Stephens, B. B., Strahan, S. E., Strode, S. A., Sweeney, C., Thames, A. B., Ullmann, K., Wagner, N., Weber, R., Weinzierl, B., Wennberg, P. O., Williamson, C. J., Wolfe, G. M., and Zeng, L.: The NASA Atmospheric Tomography (ATom) Mission: Imaging the Chemistry of the Global Atmosphere, Bulletin of the American Meteorological Society, 103, E761-E790, https://doi.org/10.1175/BAMS-D-20-0315.1, 2022.
- van der Werf, G. R., Randerson, J. T., Giglio, L., van Leeuwen, T. T., Chen, Y., Rogers, B. M., Mu, M., van Marle, M. J. E., Morton, D. C., Collatz, G. J., Yokelson, R. J., and Kasibhatla, P. S.: Global fire emissions estimates during 1997–2016, Earth Syst. Sci. Data, 9, 697–720, https://doi.org/10.5194/essd-9-697-2017, 2017.
- Vasudev, R.: Absorption spectrum and solar photodissociation of gaseous nitrous acid in the actinic wavelength region, Geophysical Research Letters, 17, 2153–2155, https://doi.org/10.1029/GL017i012p02153, 1990.
- Veres, P. R., Neuman, J. A., Bertram, T. H., Assaf, E., Wolfe, G. M., Williamson, C. J., Weinzierl, B., Tilmes, S., Thompson, C. R., Thames, A. B., Schroder, J. C., Saiz-Lopez, A., Rollins, A. W., Roberts, J. M., Price, D., Peischl, J., Nault, B. A., Møller, K. H., Miller, D. O., Meinardi, S., Li, Q., Lamarque, J.-F., Kupc, A., Kjaergaard, H. G., Kinnison, D., Jimenez, J. L., Jernigan, C. M., Hornbrook, R. S., Hills, A., Dollner, M., Day, D. A., Cuevas, C. A., Campuzano-Jost, P., Burkholder, J., Bui, T. P., Brune, W. H., Brown, S. S., Brock, C. A., Bourgeois, I., Blake, D. R., Apel, E. C., and Ryerson, T. B.: Global airborne sampling reveals a previously unobserved dimethyl sulfide oxidation mechanism in the marine atmosphere, Proceedings of the National Academy of Sciences, 117, 4505–4510, https://doi.org/10.1073/pnas.1919344117, 2020.
- Verma, S., Yadava, P. K., Lal, D. M., Mall, R. K., Kumar, H., and Payra, S.: Role of Lightning NO_x in Ozone Formation: A Review, Pure and Applied Geophysics, 178, 1425–1443, https://doi.org/10.1007/s00024-021-02710-5, 2021.

- Vinken, G. C. M., Boersma, K. F., Maasakkers, J. D., Adon, M., and Martin, R. V.: Worldwide biogenic soil NO_x emissions inferred from OMI NO₂ observations, Atmos. Chem. Phys., 14, 10363–10381, https://doi.org/10.5194/acp-14-10363-2014, 2014.
- Virtanen, P., Gommers, R., Oliphant, T. E., Haberland, M., Reddy, T., Cournapeau, D., Burovski, E., Peterson, P., Weckesser, W., Bright, J., van der Walt, S. J., Brett, M., Wilson, J., Millman, K. J., Mayorov, N., Nelson, A. R. J., Jones, E., Kern, R., Larson, E., Carey, C. J., Polat, ÿI., Feng, Y., Moore, E. W., VanderPlas, J., Laxalde, D., Perktold, J., Cimrman, R., Henriksen, I., Quintero, E. A., Harris, C. R., Archibald, A. M., Ribeiro, A. H., Pedregosa, F., van Mulbregt, P., and SciPy 1.0 Contributors: SciPy 1.0: Fundamental Algorithms for Scientific Computing in Python, Nature Methods, 17, 261–272, https://doi.org/10.1038/s41592-019-0686-2, 2020.
- Walker, J. M., Philip, S., Martin, R. V., and Seinfeld, J. H.: Simulation of nitrate, sulfate, and ammonium aerosols over the United States, Atmos. Chem. Phys., 12, 11213–11227, https://doi.org/10.5194/acp-12-11213-2012, 2012.
- Wang, L. and Zhang, J.: Detection of Nitrous Acid by Cavity Ring-Down Spectroscopy, Environmental Science & Technology, 34, 4221–4227, https://doi.org/10.1021/es0011055, 2000.
- Wang, M. and Fu, Q.: Stratosphere-Troposphere Exchange of Air Masses and Ozone Concentrations Based on Reanalyses and Observations, Journal of Geophysical Research: Atmospheres, 126, e2021JD035159, https://doi.org/10.1029/2021JD035159, 2021.
- Wang, X., Jacob, D. J., Downs, W., Zhai, S., Zhu, L., Shah, V., Holmes, C. D., Sherwen, T., Alexander, B., Evans, M. J., Eastham, S. D., Neuman, J. A., Veres, P. R., Koenig, T. K., Volkamer, R., Huey, L. G., Bannan, T. J., Percival, C. J., Lee, B. H., and Thornton, J. A.: Global tropospheric halogen (Cl, Br, I) chemistry and its impact on oxidants, Atmos. Chem. Phys., 21, 13973– 13996, https://doi.org/10.5194/acp-21-13973-2021, 2021.
- Warneke, C., Schwarz, J. P., Dibb, J., Kalashnikova, O., Frost, G., Al-Saad, J., Brown, S. S., Brewer, W. A., Soja, A., Seidel, F. C., Washenfelder, R. A., Wiggins, E. B., Moore, R. H., Anderson, B. E., Jordan, C., Yacovitch, T. I., Herndon, S. C., Liu, S., Kuwayama, T., Jaffe, D., Johnston, N., Selimovic, V., Yokelson, R., Giles, D. M., Holben, B. N., Goloub, P., Popovici, I., Trainer, M., Kumar, A., Pierce, R. B., Fahey, D., Roberts, J., Gargulinski, E. M., Peterson, D. A., Ye, X., Thapa, L. H., Saide, P. E., Fite, C. H., Holmes, C. D., Wang, S., Coggon, M. M., Decker, Z. C. J., Stockwell, C. E., Xu, L., Gkatzelis, G., Aikin, K., Lefer, B., Kaspari, J., Griffin, D., Zeng, L., Weber, R., Hastings, M., Chai, J., Wolfe, G. M., Hanisco, T. F., Liao, J., Campuzano Jost, P., Guo, H., Jimenez, J. L., Crawford, J., and Team, T. F.-A. S.: Fire Influence on Regional to Global Environments and Air Quality (FIREX-AQ), Journal of Geophysical Research: Atmospheres, 128, e2022JD037758, https://doi.org/10.1029/2022JD037758, 2023.
- Weng, H., Lin, J., Martin, R., Millet, D. B., Jaeglé, L., Ridley, D., Keller, C., Li, C., Du, M., and Meng, J.: Global high-resolution emissions of soil NO_x, sea salt aerosols, and biogenic volatile organic compounds, Scientific Data, 7, 148, https://doi.org/10.1038/s41597-020-0488-5, 2020.
- Weyland, B.: Detection of nitrous acid in the lower, middle, and upper troposphere: potential formation mechanisms of excess HONO, Ph.D. thesis, Combined Faculty of Mathematics, En-

- gineering and Natural Sciences of Heidelberg University, Germany, https://doi.org/10.11588/heidok.00034321, 2024.
- Whalley, L. K., Furneaux, K. L., Goddard, A., Lee, J. D., Mahajan, A., Oetjen, H., Read, K. A., Kaaden, N., Carpenter, L. J., Lewis, A. C., Plane, J. M. C., Saltzman, E. S., Wiedensohler, A., and Heard, D. E.: The chemistry of OH and HO₂ radicals in the boundary layer over the tropical Atlantic Ocean, Atmos. Chem. Phys., 10, 1555–1576, https://doi.org/10.5194/acp-10-1555-2010, 2010.
- Wingen, L. M., Moskun, A. C., Johnson, S. N., Thomas, J. L., Roeselová, M., Tobias, D. J., Kleinman, M. T., and Finlayson-Pitts,
 B. J.: Enhanced surface photochemistry in chloride-nitrate ion mixtures, Phys. Chem. Chem. Phys., 10, 5668–5677, 2008.
- Wofsy, S., Afshar, S., Allen, H., Apel, E., Asher, E., Barletta, B., Bent, J., Bian, H., Biggs, B., Blake, D., Blake, N., Bourgeois, I., Brock, C., Brune, W., Budney, J., Bui, T., Butler, A., Campuzano-Jost, P., Chang, C., Chin, M., Commane, R., Correa, G., Crounse, J., Cullis, P. D., Daube, B., Day, D., Dean-Day, J., Dibb, J., Di-Gangi, J., Diskin, G., Dollner, M., Elkins, J., Erdesz, F., Fiore, A., Flynn, C., Froyd, K., Gesler, D., Hall, S., Hanisco, T., Hannun, R., Hills, A., Hintsa, E., Hoffman, A., Hornbrook, R., Huey, L., Hughes, S., Jimenez, J., Johnson, B., Katich, J., Keeling, R., Kim, M., Kupc, A., Lait, L., McKain, K., Mclaughlin, R., Meinardi, S., Miller, D., Montzka, S., Moore, F., Morgan, E., Murphy, D., Murray, L., Nault, B., Neuman, J., Newman, P., Nicely, J., Pan, X., Paplawsky, W., Peischl, J., Prather, M., Price, D., Ray, E., Reeves, J., Richardson, M., Rollins, A., Rosenlof, K., Ryerson, T., Scheuer, E., Schill, G., Schroder, J., Schwarz, J., St.Clair, J., Steenrod, S., Stephens, B., Strode, S., Sweeney, C., Tanner, D., Teng, A., Thames, A., Thompson, C., Ullmann, K., Veres, P., Wagner, N., Watt, A., Weber, R., Weinzierl, B., Wennberg, P., Williamson, C., Wilson, J., Wolfe, G., Woods, C., Zeng, L., and Vieznor, N.: ATom: Merged Atmospheric Chemistry, Trace Gases, and Aerosols, Version 2, EarthData [data set], https://doi.org/10.3334/ORNLDAAC/1925, 2021.
- Wofsy, S. C., Afshar, S., Allen, H. M., et al.: ATom: Merged Atmospheric Chemistry, Trace Gases, and Aerosols (Version 1.5), ORNL Distributed Active Archive Center [data set], https://doi.org/10.3334/ORNLDAAC/1581, 2018.
- Xin, L., Rohrer, F., Hofzumahaus, A., Brauers, T., Häseler, R., Bohn, B., Broch, S., Fuchs, H., Gomm, S., Holland, F., Jäger, J., Kaiser, J., Keutsch, F. N., Lohse, I., Lu, K., Tillmann, R., Wegener, R., Wolfe, G. M., Mentel, T. F., Kiendler-Scharr, A., and Wahner, A.: Missing Gas-Phase Source of HONO inferred from Zeppelin Measurements in the Troposphere, Science, 344, 292–296, https://doi.org/10.1126/science.1248999, 2014
- Ye, C., Zhou, X., Pu, D., Stutz, J., Festa, J., Spolaor, M., Cantrell, C., Mauldin, R. L., Weinheimer, A., and Haggerty, J.: Comment on "Missing gas-phase source of HONO inferred from Zeppelin measurements in the troposphere", Science, 348, 1326–1326, https://doi.org/10.1126/science.aaa1992, 2015.
- Ye, C., Zhou, X., Pu, D., Stutz, J., Festa, J., Spolaor, M., Tsai, C., Cantrell, C., Mauldin, R. L., Campos, T., Weinheimer, A., Hornbrook, R. S., Apel, E. C., Guenther, A., Kaser, L., Yuan, B., Karl, T., Haggerty, J., Hall, S., Ullmann, K., Smith, J. N., Ortega, J., and Knote, C.: Rapid cycling of reactive nitrogen in the marine boundary layer, Nature, 532, 489–491, https://doi.org/10.1038/nature17195, 2016.

- Ye, C., Zhang, N., Gao, H., and Zhou, X.: Photolysis of Particulate Nitrate as a Source of HONO and NO_x, Environmental Science & Technology, 51, 6849–6856, https://doi.org/10.1021/acs.est.7b00387, 2017.
- Ye, C., Zhou, X., Zhang, Y., Wang, Y., Wang, J., Zhang, C., Woodward-Massey, R., Cantrell, C., Mauldin, R. L., Campos, T., Hornbrook, R. S., Ortega, J., Apel, E. C., Haggerty, J., Hall, S., Ullmann, K., Weinheimer, A., Stutz, J., Karl, T., Smith, J. N., Guenther, A., and Song, S.: Synthesizing evidence for the external cycling of NO_x in high- to low-NO_x atmospheres, Nature Communications, 14, 7995, https://doi.org/10.1038/s41467-023-43866-z, 2023.
- Yu, Y., Cheng, P., Li, H., Yang, W., Han, B., Song, W., Hu, W., Wang, X., Yuan, B., Shao, M., Huang, Z., Li, Z., Zheng, J., Wang, H., and Yu, X.: Budget of nitrous acid (HONO) at an urban site in the fall season of Guangzhou, China, Atmos. Chem. Phys., 22, 8951–8971, https://doi.org/10.5194/acp-22-8951-2022, 2022.
- Zhai, S., Jacob, D. J., Brewer, J. F., Li, K., Moch, J. M., Kim, J., Lee, S., Lim, H., Lee, H. C., Kuk, S. K., Park, R. J., Jeong, J. I., Wang, X., Liu, P., Luo, G., Yu, F., Meng, J., Martin, R. V., Travis, K. R., Hair, J. W., Anderson, B. E., Dibb, J. E., Jimenez, J. L., Campuzano-Jost, P., Nault, B. A., Woo, J.-H., Kim, Y., Zhang, Q., and Liao, H.: Relating geostationary satellite measurements of aerosol optical depth (AOD) over East Asia to fine particulate matter (PM_{2.5}): insights from the KORUS-AQ aircraft campaign and GEOS-Chem model simulations, Atmos. Chem. Phys., 21, 16775–16791, https://doi.org/10.5194/acp-21-16775-2021, 2021a.
- Zhai, S., Jacob, D. J., Wang, X., Liu, Z., Wen, T., Shah, V., Li, K., Moch, J. M., Bates, K. H., Song, S., Shen, L., Zhang, Y., Luo, G., Yu, F., Sun, Y., Wang, L., Qi, M., Tao, J., Gui, K., Xu, H., Zhang, Q., Zhao, T., Wang, Y., Lee, H. C., Choi, H., and Liao, H.: Control of particulate nitrate air pollution in China, Nature Geoscience, 14, 389–395, https://doi.org/10.1038/s41561-021-00726-z, 2021b.
- Zhang, Y., Sun, J., Shen, X., Lal Chandani, V., Du, M., Song, C., Dai, Y., Hu, G., Yang, M., Tilstone, G. H., Jordan, T., Dall'Olmo, G., Liu, Q., Nemitz, E., Callaghan, A., Brean, J., Sommariva, R., Beddows, D., Langford, B., Bloss, W., Acton, W., Harrison, R., Dall'Osto, M., and Shi, Z.: Measurements of particulate methanesulfonic acid above the remote Arctic Ocean using a high resolution aerosol mass spectrometer, Atmospheric Environment, 331, 120538, https://doi.org/10.1016/j.atmosenv.2024.120538, 2024.

- Zhao, Y., Saunois, M., Bousquet, P., Lin, X., Berchet, A., Hegglin, M. I., Canadell, J. G., Jackson, R. B., Hauglustaine, D. A., Szopa, S., Stavert, A. R., Abraham, N. L., Archibald, A. T., Bekki, S., Deushi, M., Jöckel, P., Josse, B., Kinnison, D., Kirner, O., Marécal, V., O'Connor, F. M., Plummer, D. A., Revell, L. E., Rozanov, E., Stenke, A., Strode, S., Tilmes, S., Dlugokencky, E. J., and Zheng, B.: Inter-model comparison of global hydroxyl radical (OH) distributions and their impact on atmospheric methane over the 2000–2016 period, Atmos. Chem. Phys., 19, 13701–13723, https://doi.org/10.5194/acp-19-13701-2019, 2019.
- Zhao, Y., Saunois, M., Bousquet, P., Lin, X., Hegglin, M. I., Canadell, J. G., Jackson, R. B., and Zheng, B.: Reconciling the bottom-up and top-down estimates of the methane chemical sink using multiple observations, Atmos. Chem. Phys., 23, 789–807, https://doi.org/10.5194/acp-23-789-2023, 2023.
- Zhong, X., Shen, H., Zhao, M., Zhang, J., Sun, Y., Liu, Y., Zhang, Y., Shan, Y., Li, H., Mu, J., Yang, Y., Nie, Y., Tang, J., Dong, C., Wang, X., Zhu, Y., Guo, M., Wang, W., and Xue, L.: Nitrous acid budgets in the coastal atmosphere: potential daytime marine sources, Atmos. Chem. Phys., 23, 14761–14778, https://doi.org/10.5194/acp-23-14761-2023, 2023.
- Zhu, C., Xiang, B., Chu, L. T., and Zhu, L.: 308 nm Photolysis of Nitric Acid in the Gas Phase, on Aluminum Surfaces, and on Ice Films, The Journal of Physical Chemistry A, 114, 2561–2568, https://doi.org/10.1021/jp909867a, 2010.
- Zhu, Y., Wang, Y., Zhou, X., Elshorbany, Y. F., Ye, C., Hayden, M., and Peters, A. J.: An investigation into the chemistry of HONO in the marine boundary layer at Tudor Hill Marine Atmospheric Observatory in Bermuda, Atmos. Chem. Phys., 22, 6327–6346, https://doi.org/10.5194/acp-22-6327-2022, 2022.